Published in final edited form as:

Neurobiol Dis. 2015 May ; 77: 191–203. doi:10.1016/j.nbd.2015.03.005.

Interrogating the Aged Striatum: Robust Survival of Grafted Dopamine Neurons in Aging Rats Produces Inferior Behavioral Recovery and Evidence of Impaired Integration

Timothy J. Collier[1,*], **Jennifer O'Malley**[2,*], **David J. Rademacher**[3], **Jennifer A. Stancati**[1], **Kellie A. Sisson**[1], **Caryl E. Sortwell**[1], **Katrina L. Paumier**[1], **Kibrom G. Gebremedhin**[1], and **Kathy Steece-Collier**[1]

[1]Michigan State University, College of Human Medicine, Department of Translational Science and Molecular Medicine & The Udall Center of Excellence in Parkinson's Disease Research, 333 Bostwick Ave NE, Grand Rapids, Michigan, 49503

[2]Cincinnati Children's Hospital Medical Center, Division of Child Neurology, 3333 Burnet Avenue, Cincinnati, OH 45229

[3]Lake Forest College, Department of Psychology, 555 N Sheridan Rd, Lake Forest, IL 60045

Abstract

Advanced age is the primary risk factor for Parkinson disease (PD). In PD patients and rodent models of PD, advanced age is associated with inferior symptomatic benefit following intrastriatal grafting of embryonic dopamine (DA) neurons, a pattern believed to result from decreased survival and reinnervation provided by grafted neurons in the aged host. To help understand the capacity of the aged, parkinsonian striatum to be remodeled with new DA terminals, we used a grafting model and examined whether increasing the number of grafted DA neurons in aged rats would translate to enhanced behavioral recovery. Young (3 mo), middle-aged (15 mo), and aged (22 mo) parkinsonian rats were grafted with proportionately increasing numbers of embryonic ventral mesencephalic (VM) cells to evaluate whether the limitations of the graft environment in subjects of advancing age can be offset by increased numbers of transplanted neurons. Despite robust survival of grafted neurons in aged rats, reinnervation of striatal neurons remained inferior and amelioration of levodopa-induced dyskinesias (LID) was delayed or absent. This study demonstrates that: 1) counter to previous evidence, under certain conditions the aged striatum can support robust survival of grafted DA neurons; and 2) unknown factors associated with the aged

Address correspondence to: Kathy Steece-Collier, Ph.D., Department of Translational Science & Molecular Medicine, Michigan State University, 333 Bostwick Avenue NE, Grand Rapids, MI 49503; ph: 616-234-0969; fax: 616-234-0990; kathy.steece-collier@hc.msu.edu.

*These authors contributed equally to this work.

Conflict of Interest

The authors declare no competing financial interests.

striatum result in inferior integration of graft and host, and continue to present obstacles to full therapeutic efficacy of DA cell-based therapy in this model of aging.

Keywords

Parkinson's disease; aging; rodent; grafting; dyskinesias; levodopa; synaptopodin

Introduction

The therapeutic potential of dopamine (DA) neuron grafts in patients with Parkinson's disease (PD) has been variable and remains controversial and incompletely understood. Despite a moratorium on clinical grafting in PD over the previous decade, a critical reappraisal of preclinical and clinical transplantation data has lead to a limited renewal of clinical trials (Barker et al., 2013; ClinicalTrials.gov NCT01898390). This, together with continuing interest in stem cell-based replacement strategies (Ambasudhan et al., 2014; Buttery & Barker, 2014; Sundberg & Isacson, 2014) and trophic factor-induction of nigral DA terminal re-growth (Kordower & Bjorklund, 2013; Hickey & Stacy, 2013), highlights the importance of understanding the capacity and limitations of repairing the parkinsonian striatum. In addition to implications for clinical application of DA neuron grafting, cell transplantation is a valuable approach for interrogating the nature of the environment of the aged brain as it permits or discourages integration of new elements intended to facilitate restoration and repair. The presence of grafted cells, in effect, reveals characteristics of the environment through their attempts to survive, grow, and integrate with the host brain.

While clinical and preclinical data support the idea that DA neuron transplantation into the striatum is most effective in younger individuals (Collier et al., 1999; Freed et al., 2001; Sortwell et al., 2001) with less severe DA-depletion (Breysse et al., 2007; Piccini et al., 2005), clinical grafting trials to date have enrolled primarily patients with advanced PD that were not benefiting from standard medical therapy (Evans et al., 2012; Kefalopoulou et al., 2011; Ma et al., 2011). The rationale for choosing this population of patients is valid in that these individuals represent the population most in need of alternative therapeutics; nevertheless, the impact of factors associated with the environment of the severely DA-depleted, aged striatum on the overall success of previous cell transplantation trials in PD remains incompletely understood.

There have been painstaking efforts both in the clinic and the laboratory to characterize optimal donor cells used for cell transplantation therapy in PD, addressing issues including the source material for grafted cells, donor cell age, density of cell grafts, immune factors, and growth factors (e.g.: Sladek et al., 1998; Collier et al., 1999; Freed et al., 2001; Toledo-Aral et al., 2003; Terpstra et al., 2007; Soderstrom et al., 2008; Bjorklund & Kordower, 2013). However, comparatively little has been done to determine the impact of the host environment on transplant success, with most of the attention given to defining the optimal transplant location (Stromberg et al., 1986; Goren et al., 2005; Breysse et al., 2007). In humans (Freed et al., 2001) and in rats (Collier et al., 1999; Breysse et al., 2007) grafting into aged parkinsonian subjects is significantly less effective in providing behavioral benefit

than grafting in their younger counterparts. It has long been known that the aged brain lacks many support factors found in younger brains (Collier et al., 1999; 2005; Ling et al., 2000), and is generally considered to be an impoverished or hostile environment for grafted embryonic neurons. Many researchers continue to explore methods of increasing survival of grafted DA neurons for PD (e.g.: Buchele et al., 2014; Chermenina et al., 2014; Battista et al., 2014; Timmer et al., 2014), irrespective of host age. However, the purpose here was to determine if cell replacement therapy in the aged parkinsonian rat is equally therapeutic as in a younger cohort when the challenge of limited survival of grafted cells is overcome.

Previous data from our laboratories (Collier et al., 1999[1]; Sortwell et al., 2001[2]) has indicated that when the same number (i.e.: 200,000[1] or 300,000[2]) of embryonic rat ventral mesencephalic (VM) cells are grafted into striatum of parkinsonian rats of varying ages, there is a proportional decrease in survival of engrafted DA neurons with increasing host age. This reduced survival of grafted DA neurons is associated with diminished reinnervation of the striatum, and blunted recovery of asymmetric rotational behavior (Collier et al., 1999). In an attempt to achieve an equivalent number of surviving grafted neurons across host ages, we extrapolated cell survival data from our previous study (Collier et al., 1999) and grafted two-fold or five-fold the number of VM cells into 15- or 22-month-old parkinsonian rats, respectively, compared to their 3 month-old counterparts. Numbers of surviving grafted neurons and their pattern of reinnervation were evaluated. The behavioral efficacy of embryonic VM grafts was evaluated using amphetamine-induced rotational behavior and amelioration of levodopa-induced dyskinesias (LID). The results from this study suggest that even when increased survival of grafted neurons and increased neurite outgrowth is achieved for all aging parkinsonian subjects, yet-to-be-identified factors in the aged, parkinsonian brain continue to limit the behavioral efficacy of graft integration and function. While significant recovery of rotational behavior is achieved, improvements in the more complex repertoire of levodopa-induced dyskinetic behaviors are delayed or absent in the aged host.

Materials and methods

Animals

Fischer-344 (F344) rats (Harlan, Indianapolis, IN, USA) were housed in groups of three with *ad libitum* access to food and water in their home cages. Three age groups of rats were studied: (1) young adult rats (3 months old at time of the lesion, N=8, sham or DA graft), (2) middle-aged rats (15 months old at time of the lesion, N=15, sham or DA graft), and, (3) aged rats (22 months old at time of the lesion, N=15, sham or DA graft). Rats were maintained on a 12 h light: dark cycle with lights on at 0700. All studies were carried out in accordance with the Declaration of Helsinki and with the Institute for Laboratory Animal Research of the National Academy of Science *Guide for the Care and Use of Laboratory Animals* and were approved by The Institutional Animal Care and Use Committee at University of Cincinnati, where the studies were carried out. All efforts were made to minimize the number of animals used and to avoid pain or discomfort.

Experimental design overview

The experimental timeline is shown in Figure 1. Briefly, rats were rendered parkinsonian via unilateral stereotaxic injection of 6-hydroxydopamine (6-OHDA) into the substantia nigra and medial forebrain bundle. Two weeks after 6OHDA surgery, rats were evaluated for lesion success with amphetamine-induced rotational behavior. One week later (3 weeks post-surgery), rats were primed with levodopa for 4 weeks prior to grafting. Seven weeks after lesioning, and four weeks into levodopa treatment, parkinsonian rats from each age group received an intrastriatal embryonic day 14 (E14) ventral mesencephalic (VM) or a sham (cell-free media) graft. Rats were withdrawn from levodopa for one week following graft surgery (Lee et al., 2000; Steece-Collier et al., 2003; Maries et al., 2006) and reinitiated thereafter. All parkinsonian rats were evaluated for levodopa-induced dyskinesias (LID) behaviors prior to and following grafting (Figure 1). Eleven weeks after graft surgery, functional benefit was assessed with amphetamine-induced rotational behavior, with levodopa withdrawn for 48 hours prior amphetamine. Rats were sacrificed 24 hours after this final amphetamine behavioral assessment. Details of surgical procedures, behavioral evaluations and drug treatments are provided in the following paragraphs.

6-OHDA Lesion Surgery

F344 rats received unilateral stereotaxic injections of 6-OHDA into both the left medial forebrain bundle (MFB) and left substantia nigra (SN). The SN coordinates were 4.8 mm posterior to bregma, 1.7 mm lateral to mid-saggital suture, and 8.0 mm below the skull surface (Paxinos and Watson, 1998). MFB coordinates were 4.3 mm posterior to bregma, 1.2 mm lateral to mid-saggital suture, and 8.0 mm below the skull surface. Animals were anesthetized prior to surgery with an intraperitoneal (i.p.) injection of chloropent (3.0 ml/kg body weight; chloral hydrate, 42.5 mg/ml + sodium pentobarbital, 8.9 mg/ml) and placed in a stereotaxic frame. The neurotoxin solution (5μg 6-OHDA hydrobromide/μl 0.9% sterile saline containing 0.2 mg/ml ascorbic acid) was injected at a rate of 0.5 μl/min (2.0 μl total at each site) using a 5 μl Hamilton syringe with a 26-gauge needle.

Amphetamine-induced rotational behavior

Amphetamine-induced rotational asymmetry was examined at 2 weeks after the 6-OHDA surgery to confirm the presence of an adequate lesion, and 11 weeks after graft surgery to assess behavioral efficacy of neural grafts (Figure 1). Rats were injected with amphetamine sulfate (5.0 mg/kg, i.p.) and rotational behavior was monitored for 90 min using automated rotometers (TSE Systems, Germany). Rats rotating, prior to transplantation, at a rate of ≥7 ipsilateral turns per minute over 90 min were included in this study. Our lab has previously confirmed that rats with this rotational rate have >95% SN DA neuron loss and striatal DA depletion and readily develop LID (Maries et al., 2006; Steece-Collier et al., 2003).

Levodopa administration

Three weeks after a 6-OHDA lesion, but prior to grafting, animals were injected once daily with levodopa to induce abnormal involuntary dyskinetic behaviors, or LID. Subjects were first primed with once daily (Monday thru Friday) levodopa at a dose of 25 mg/kg levodopa plus 25 mg/kg benserazide (intraperitoneal (i.p.)) for one week. Subsequently, rats received

a daily maintenance dose of 12.5 mg/kg levodopa plus 12.5mg/kg benserazide for the remainder of the experiment, both pre- and post-grafting as depicted in Figure 1. Levodopa was injected at the same time daily (M-Fr).

All rats were given a 7-day levodopa-free period following grafting to prevent any interactions of the drug with the VM neuron grafts (Lee et al., 2000; Steece-Collier et al., 2003; Maries et al., 2006). One week after transplantation, rats resumed their daily levodopa treatment regimen (12.5 mg/kg levodopa plus 12.5 mg/kg benserazide, i.p.).

Dyskinesia rating

The terms “dyskinesia” and “LID” are used throughout the text to refer to abnormal involuntary movements including dystonia, hyperkinesia, and/or stereotypies noted in parkinsonian rats in response to levodopa. The details of these behaviors and the rating scale used are reported elsewhere (Steece-Collier et al., 2003; Maries et al., 2006). Dyskinetic behaviors were rated three days per week (Wednesday-Friday) for 2 min each day, 30 minutes after the levodopa injection, a time that corresponds to peak dose dyskinesias (e.g.: Maries et al., 2006). Injections were timed such that each animal was rated precisely 30 min after their levodopa injection. Dyskinesia ratings were performed by the same individual throughout the study. This investigator was blinded to the treatment conditions and checked weekly with inter-rater reliability by a second blinded investigator. Dyskinesia ratings for all the animals were carried out in randomized order, assigned at the beginning of the experiment and kept for the duration. As detailed previously (Steece-Collier et al., 2003; Maries et al., 2006) both the intensity (0= absent, 1= mild, 2= moderate, 3= severe) and frequency (0= absent, 1= <50% of rating period, 2= 50% of the rating period, 3= constant) were determined for the following individual dyskinetic behaviors: forelimb hyperkinesia, forelimb dystonia, hind limb dystonia, trunk dystonia, neck dystonia, and orolingual dyskinesia. A final dyskinesia severity score for any given individual component of dyskinesia was obtained by multiplying frequency × intensity. A total daily severity score for each animal was computed by adding the severity scores of the individual dyskinetic behaviors. A total weekly LID score for each animal was computed by averaging the daily severity score for Wednesday through Friday. Post-graft LID behaviors are represented in graphs as temporal categories of ‘early’, ‘middle’, and ‘late’. A modified bootstrapping method was used to assign these categories and for the analysis of behaviors that had extensive temporal data (i.e.: Figures 7, 8). This approach involved the inclusion of re-sampled data from the following time-point groupings: ‘early’ time-point (weeks 2–4 wks post-grafting); ‘middle’ time-point (weeks 6–8 wks post-grafting); and a ‘late’ time-point (weeks 10–11 wks post-grafting). Figures of individual LIDs (dystonia in trunk and forepaw (RFPD), dyskinesia in forepaw and hindpaw, and orolingual dyskinesia) are presented for each age group compared to a reference plot of combined behaviors for sham-grafted subjects of all age groups as these data were not statistically different.

Preparation of donor tissue for transplantation

VM tissue containing developing A8-A10 DA cell groups was dissected from E14 F344 rats (crown-rump length 10.0–11.5 mm). VM tissue was collected and pooled in 4°C calcium–magnesium free (CMF) buffer. Tissue was then transferred to CMF buffer containing 0.1%

trypsin, warmed to 37°C in a water bath for 10 min, rinsed in CMF buffer, and triturated in 0.004% DNase using Pasteur pipettes of 1.0 mm and 0.5 mm tip diameter. The resulting suspension was pelleted by centrifugation at 500 × *g* for 10 min. The pellet was suspended in 1.0 ml of Neurobasal Media (Gibco). This media in the absence of cells served as the vehicle for sham grafting. The trypan blue exclusion test was used to estimate cell number and viability. Final suspensions were prepared at a density of 33,333 cells/ ſl for young (3 mo) rats; 66,666 cells/ ſl for middle-aged (15 mo) rats, and 150,000 cells/ ſl for aged (22 mo) rats according to the design detailed below. Cells were kept on wet ice during transplantation surgery and used within 4 hours of preparation.

Cell transplantation

Rats were assigned to sham and VM graft groups such that the groups had an equal distribution of pre-graft LID severity and amphetamine-induced rotational scores. VM grafted animals received embryonic VM cells at a single striatal site (anterior to bregma +0.2mm; lateral to bregma +2.8mm; Paxinos and Watson, 1998), with tissue dispersed along three dorsal-ventral locations at this site: 5.8, 5.1 and 4.4 mm ventral to dura. The number of grafted VM cells was varied between age groups in an attempt to achieve an equal final number of surviving DA neurons in the VM graft across the age groups. These numbers were derived from our previous study (Collier et al., 1999) where we found that the survival of grafted DA neurons in middle-aged parkinsonian rats (17 mo) was one-half of that noted in young (4 mo) rats, and the survival of grafted DA neurons in aged parkinsonian rats (24–26 mo) was one-fifth of that noted in young rats. Due to a predicted 50% reduction in cell survival in middle-aged rats, 15 month-old rats received 400,000 VM cells/animal. Similarly, due to a predicted five-fold reduction in cell survival in advanced-aged rats, 22 month old rats received a total of 900,000 VM cells/rat. The embryonic VM cell suspension was delivered into the DA-depleted striatum using a 10 ſl Hamilton syringe with a 26-gauge needle. Each dorsal-ventral injection site received 2 ſl of the VM cell suspension for a total volume of 6 ſl for all rats. Sham-grafted subjects received injections of 6µl of cell-free vehicle using the same stereotaxic coordinates. The needle was left in place for three minutes after the last injection of cells or media.

Necropsy

Following the eleventh week after grafting, rats were deeply anesthetized then perfused transcardially with room temperature heparinized 0.9% saline (150 ml) followed by buffered fresh 4.0% paraformaldehyde solution (100ml). Brains were post-fixed for 24 hours in 4.0% paraformaldehyde solution at 4°C followed by transfer to a 30% sucrose solution for 48–72 hours. Coronal brain sections were cut on a freezing sliding microtome at 40 ſm thickness, and all sections were stored at −20°C in a cryoprotectant solution until time of processing.

Immunohistochemistry

Paraformaldehyde-fixed sections through the striatum were used for immunohistochemical (IHC) staining of tyrosine hydroxylase (TH; marker for DA neurons) (Kordower et al., 1995; Steece-Collier et al., 1995), FosB/ΔFosB (FosB; marker for LID-related immediate early gene activation), a dopamine and cAMP regulated phosphoprotein 32 kDa

(DARPP-32; marker for striatal medium spiny neurons (MSNs) and used as a marker of striatal cytoarchitectural integrity) and synaptopodin (SP; a dendritic spine apparatus associated protein and used to measure the number of (presumed) synaptic contacts between TH+ neurites and host MSNs). A separate series of every sixth section through the striatum were stained for each of these antibodies. For TH IHC, sections were incubated with TH primary antibody (1:4000; EMD Millipore, Billerica, MA) for 24 hours at room temperature followed by 90 minutes in goat anti-mouse biotinylated IgG (1:400; EMD Millipore, Billerica, MA) and developed using 0.05% 3,3'-diaminobenzadine (DAB). For DARPP-32 IHC tissue was incubated overnight at room temperature in monoclonal DARPP-32 primary antibody (1:10000; Cell Signaling Technology) followed by incubation for one hour in goat anti-rabbit IgG (1: 400, EMD Millipore, Billerica, MA) and developed using DAB. For FosB IHC, sections through the striatum were incubated overnight at room temperature in an antibody against FosB/ΔFosB isoforms (1:2000, Santa Cruz Biotech, CA), followed by incubation in biotinylated goat℃anti rabbit IgG (Vector Laboratories, Burlingame, CA) at a concentration of 1:200 in TBS containing 1% goat serum for 90 min at room temperature. Sections were developed using the avidin℃biotin℃peroxidase complex (ABC) (Vector Laboratories, Burlingame, CA) and DAB. Sections were mounted on gelatin-coated slides, dehydrated, and cover slipped. The slides were visualized using light microscopy.

For fluorescent dual-label TH-SP IHC, sections were incubated for 48 hours at room temperature in mouse anti-TH (1:8000; Millipore) plus rabbit anti-SP (1:4000; Synaptic Systems). After several rinses, sections were then incubated with donkey anti-mouse IgG (1:400; Alexa Fluor 488 (green); Invitrogen) plus donkey anti-rabbit IgG (1:400; Alexa Fluor 594 (red); Invitrogen) for 90 minutes at room temperature in the dark. Sections were mounted onto Histobond® slides, dipped into a Sudan Black solution (to reduce autofluorescence; 1g/50ml 70% ethanol), rinsed with 70% ethanol and coverslipped in the dark with ProLong® Gold Anti-Fade reagent (Life Technologies). Slides were visualized using confocal microscopy. For all antibodies, controls consisted of processing tissue in an identical manner except for omitting the primary antibody.

Stereological quantification of graft cell number

The number of grafted TH-immunoreactive (THir) cells located within the striatum was estimated using an optical dissector sampling design by an investigator blinded to the grafting conditions (Gundersen et al., 1988; Kordower et al., 2001; Larsen et al., 2004). Three to five equally-spaced sections were sampled along the entire rostral-caudal extent of the graft for each brain. The region of the graft was outlined using a 4X objective. A systematic sample of the area occupied by the graft was made from a random starting point determined by the software (StereoInvestigator 2000 software; MBF Bioscience, Colchester, VT). The counting frame was established at 50×50 ƒm such that the number of sampling sites covered the entire area of the graft within each section, without overlap, or gaps, thus enabling complete enumeration of the analyzed tissue. These parameters resulted in ~700–1400 sample sites per section. Counts of THir cells were made at regular predetermined intervals (x=50 ƒm, y=50 ƒm), and a counting frame (50×50μm=2500 $ƒm^2$) was superimposed on the image of the tissue sections. These sections were then analyzed using a 60X Plan Apo oil immersion objective. The measured section thickness averaged

approximately 24 ƒm. The optical dissector height was 20 ƒm. This method allowed for guard zones of 2 ƒm on either surface of the tissue sample, such that cell counting was conducted only within the optical dissector. THir cells were only counted if the first recognizable labeled profiles of the cell came into focus within the counting frame (Gundersen et al., 1988 a,b; Larsen et al., 2004). The percent of grafted THir neuron survival was based on approximately 200,000* cells per VM obtained with our dissection parameters and calculated as:

Total # of THir Neurons Implanted = Total # of VM cells grafted per age group (i.e.: 200,000, 500,000, 900,000) × (37,500 THir Neurons/200,000* cells per VM).

% Survival Rate = (Stereological Mean of surviving THir neurons in graft of each age group/ Total # of THir Neurons Grafted) × 100 (for details see Terpstra et al., 2007).

Graft volume quantification

Striatal and graft volumes were calculated using the Neurolucida® stereology program (MBF Bioscience, Williston, Vermont). Briefly, contours were defined for both the striatum and the graft, and the outlines of each structure were traced in THir sections throughout the entire length of the striatum. The same brain sections used for graft cell counts were used for graft volume analysis. The Neurolucida Explorer program was used to calculate total graft and striatal volume for each animal.

Quantification of neurite outgrowth

The extent of graft-derived innervation of the host striatum was evaluated with two methods: densitometry of THir fiber immunoreactivity surrounding the graft, and stereology using the Space Balls program (MBF Bioscience) in a selected region adjacent to the graft. Densitometric measurements were performed using the Nikon NIS-Elements software to assess THir neurites in multiple fields of view extending from the dorsal, ventral, lateral, and medial borders of the grafts (Figure 3B). Measurements are expressed as the “Area Fraction,” which represents the percentage of the field of view occupied by THir fibers. All fields of view for all animals were set to identical light settings on the microscope and identical threshold levels to subtract background staining. Background readings were taken from multiple fields of view within the corpus callosum for each animal to establish this threshold before data collection began. The investigator was blinded to the age and treatment conditions of each animal before data collection. For each animal, the dorsal, medial, ventral, and lateral borders of the graft were identified under the microscope (Figure 3). The tissue section containing the largest portion of graft was chosen for analysis for each animal. Beginning at the dorsal border of the graft, images were acquired at 40X as consecutive adjacent fields of view, with no overlap between regions. This resulted in each field of view representing a total area of 281.60μm × 225.28μm. Images were collected from the border of the graft to the corresponding striatal border (e.g.: the dorsal border of the graft to the dorsal border of the striatum), resulting in data from 3–12 fields of view for any given direction, which varied based on graft placement. The first six fields of view extending from the graft border in each direction were used for final analyses as reliable detection of staining was reduced beyond this distance. Data was analyzed for neurite extension proximal

to the graft (1–3 fields of view from graft border) and distal to the graft (4–6 fields of view from graft border) in each measured axis (dorsal, medial, ventral, and lateral), for young, middle-aged, and aged VM grafted rats (Figure 3).

Fiber density analyses were also performed utilizing the Space Balls stereological probe to obtain an unbiased estimate of THir neurite densities in the striatum based on previously reported methods (Thompson et al., 2012). Contours were drawn for three fields of view matching the dimensions of the fields of view used for the densitometry analysis at the lateral border of the graft. Contours of the same side were drawn on the intact side to collect fiber density for the intact side of each rat. The same section of grafted tissue analyzed in the densitometry analysis was used for analysis via the Space Balls software. Neurites were counted using a BX52 Olympus microscope (Olympus America Inc.) equipped with a Microfire CCD camera (Optronics). The camera settings were maintained throughout the entirety of each experiment and the investigator was blinded to the treatment conditions during the analysis.

Striatal integrity

DARPP-32 is expressed in all striatal medium spiny neurons (MSNs) (Ouimet et al., 1998) and thus is a commonly used MSN marker. The volume of striatal displacement under all grafting conditions (e.g. VM or sham) was assessed via DARPP-32-ir staining of the striatum in each experimental subject. As with graft volume measurement, striatal outlines were traced throughout the striatum in its entirety using the Neurolucida® stereology program for volume assessment (MBF Bioscience, Williston, Vermont). The area devoid of DARPP-32 staining was clearly demarcated in 3–5 sections of the striatum for all subjects, corresponding to the VM graft or sham-graft area. This striatal area was traced to give a contour specific for the striatal area devoid of DARPP-32 immunoreactivity. The total volume of striatum expressing DARPP-32 was quantified as the difference between total striatal volume and volume of the area devoid of DARPP-32 immunoreactivity (i.e.: percent total striatum with positive DARPP-32 staining).

Densitometry analysis of FosB/ΔFosB immunoreactive cells

Three sections of the dorsolateral precommissural striatum were analyzed for FosB/ΔFosB staining in each animal by an investigator blinded to the experimental treatment. Tissue sections selected for analysis corresponded to (1) pre-graft striatum, (2) the first rostral section containing the grafted striatum, and (3) the following section, immediately adjacent to the previous one containing grafted THir cells. Slides were visualized at a magnification of 40X using light microscopy (Olympus BX60, Olympus, USA) and were digitized using a Nikon DM1200 camera and ACT software (Nikon Microscopy, USA). At each of the three striatal levels, two sampling images were obtained for both the DA-depleted and intact striatum. The first image of striatal FosB/ΔFosB positive cells was obtained adjacent to the lateral border of the striatum at a mid-dorsoventral level. The second imaged area was of the same size, adjacent and just medial to the first area. Densitometry of FosB/ΔFosB-ir cells within the digitized images was performed using ImageJ software (National Institutes of Health, Bethesda, Maryland). The investigator blinded to the experimental conditions outlined each of the FosB/ΔFosB-positive cells in the digitized images, with the optical

density of each cell then being measured by the computer software. A mean optical density reading was generated for each immunoreactive cell. An average of 50 cells was sampled per field of view yielding 300 cells per animal per side. An average optical density was calculated for all FosB/ΔFosB-ir cells present in the two adjacent field of view images. The background level of optical density was determined by tracing areas consisting of internal capsule fibers within the striatum located between the FosB/ΔFosB-ir cells. An average background optical density value was obtained from a total of 60 of these regions per animal per side. The corrected FosB/ΔFosB optical density was obtained by subtracting the average background optical density from the average optical density obtained for the FosB/ΔFosB-ir cells. The optical density of the FosB/ΔFosB-positive cells present in the dorsolateral lesioned striatum at each level was expressed as a percent increase from the value found in the unlesioned (intact) striatum at the same level.

Quantification of contact between TH+ neurites and SP+ elements

An investigator blinded to treatment conditions analyzed the number of SP+ contacts per length of TH+ neurite (number of contacts/fiber length measured). The tissue section containing the largest portion of the graft was chosen for analysis of SP–TH appositions in each animal. As depicted in Figure 3B, at the equator, on the medial aspect of the graft, data was collected in two fields of view (FOV) (with each FOV equal to 125 μm using the 100X objective). Slides were visualized and photographed at 100X using an Olympus FluoView FV1000 Confocal Laser Scanning Microscope (Olympus America, Inc., Center Valley, PA). Images were digitized using Olympus Fluoview FV1000 Advanced Software (version 3.01). Digitized micrographs were analyzed using Olympus Fluoview Viewer (version 4.0a). Approximately 20 TH+ fiber segments of at least 10 um were identified in each image. The criteria for selecting SP+ labeling was that the SP element should have direct contact with the TH+ fiber, should show bright immunofluorescence, and have well-defined edges.

Statistical analysis

Dyskinetic behaviors were analyzed using three-way analysis of variance (ANOVA) employing Sigma Stat 3.0 software (Aspire Software International, Leesburg, VA) to determine if there were significant between age-groups differences in the severity of LIDs and the behavioral efficacy of the grafts. Student-Newman-Keuls (SNK) tests were used for multiple comparisons when there was a significant ANOVA. An ANOVA followed by SNK tests were also used to determine if there were significant differences between sham and VM grafts, and determine if host age had a significant effect on the survival of grafted TH-ir cell counts, VM graft volume, and ability of TH-ir cells to normalize optical density of the FosB/ΔFosB marker. Two-way ANOVAs were used to determine statistical differences in neurite outgrowth, followed by the SNK post-hoc test. One-way ANOVA followed by SNK tests were used to analyze the synaptopodin and TH data. The level of statistical significance was set at $p<0.05$ for all statistical analyses.

Results

Increasing the number of VM cells grafted into aged rats results in a proportional increase in grafted THir cell survival

In contrast to expectations based on previous findings (Collier et al., 1999; Sortwell et al., 2001) when the number of VM cells grafted into middle-aged and aged rats was increased, the number of surviving THir neurons in the striatum at 11 weeks after grafting was significantly greater than in their younger counterparts (total number of grafted THir cells: young: 1,505.67 ± 590.56; middle-aged: 3,250.86 ± 616.97; aged: 5,261.50 ± 989.09; $F(2,15)=4.18$, $p=0.040$, Figure 2). However, the overall percentage of grafted THir neuron survival did not vary significantly across age (young: 4.02% ± 1.58; middle-aged: 3.45% ± 0.66; aged: 3.12% ± 0.59; $F(2,15)=0.24$, $p=0.788$).

Stereological quantification of graft volume showed that middle-aged and aged graft recipients had significantly larger graft volumes as compared to their younger counterparts corresponding to the significantly larger number of grafted cells (young: 0.16 ± 0.02 mm^3; middle-aged: 0.46 ± 0.09mm^3; aged: 0.83 ± 0.31mm^3; $F(2,16)=6.65$, $p=0.009$, Figure 3A).

Graft-derived reinnervation is not proportional to increased survival of grafted neurons in aging hosts

The area of striatum occupied by graft-derived neurites was similar in host animals of varying ages. When analyzed as a composite of both proximal and distal FOV occupied by neurites along the four points of the compass at the center of the graft, there was overlap across all three age groups. When THir neurite density was expressed as percent FOV for regions either proximal or distal to the graft, the larger number of surviving grafted THir neurons in middle-aged and aged subjects was associated with increased graft-derived innervation immediately adjacent (proximal) to the implant (Figure 3 C, D). In addition, composite neurite density measures using the Space Ball probe were not significantly different among groups ($F(2,26)=3.17$, $p>0.05$). This equivalency in reinnervation in the areas sampled does not account for the significantly different numbers of grafted cells contributing the innervation. When the extent of reinnervation is expressed relative to the number of surviving grafted THir neurons, a dramatic decline in neurite density per cell is detected beginning in middle-age and persisting in old age ($F(2,26)=4.54$, $p=0.02$; young vs middle $p=0.02$, young vs aged $p=0.04$, middle vs aged $p=0.98$; Figure 4). Thus, while equivalent graft-derived innervation of the striatum can be achieved in subjects of advancing age, it requires many more grafted neurons to do so. The limitation of neurite density in the aged rats did not appear related to a ‘ceiling effect’ as the mean neurite density was significantly greater on the intact side versus the DA-grafted side for all age groups (average neurite outgrowth: intact: 0.156 +/− 0.010 um/mm^3; graft: 0.053+/− 0.010um/mm^3; $p< 0.001$, $F = 54.7$) with the aged DA-grafted striatum reaching a maximum of only 41.6% the neurite density found in the intact striatum. Further, there was no age-dependent difference in neurite density between the intact versus DA grafted striata (average neurite density: young intact = 0.172 ± 0.018 um/mm^3; middle intact = 0.149 ± 0.018um/mm^3; aged intact = 0.149 ± 0.0128um/mm^3; young grafted = 0.043 ± 0.018; middle grafted = 0.053 ± 0.018; aged grafted = 0.062 ± 0.018; $P = 0.466$; $F = 0.811$).

Striatal neuron cytoarchitecture is equally preserved in the grafted striatum across all ages

Striatal DARPP-32 immunoreactivity revealed a normal appearance of the gross cytoarchitecture throughout the majority of the grafted striatum across all age groups. Specifically there was a distinct localized area devoid of DARPP-32 staining in all grafted animals corresponding to the presence of the implant (Figure 5). Despite the difference between age groups in the number of grafted THir neurons and the volume of striatum they occupied, there was no age-related difference in the volume of striatum staining for DARPP-32 (VM grafted rats: young 99.85% ± 0.86%; middle-aged 98.30% ± 0.57%; aged 96.93% ± 0.47%; % of striatal volume with DARPP-32-ir; $F(2,36)=1.18$, $p>0.05$) and equivalent to the volume of DARPP-32 staining in sham-grafted rats (sham-grafted rats: young 99.97% ± 0.75%; middle-aged 99.95% ± 0.53%; aged 99.97% ± 0.67%). While dyskinogenic levodopa can change the phosphorylation of DARPP-32 at Thr34 (Santini et al., 2007), there was no effect on level of DARPP-32 immunoreactivity as a marker of MSN number as observed in the lesioned, sham-grafted striata. Accordingly, in both the sham-grafted and VM grafted striatum, greater than 96% of the region showed normal DARPP-32 immunostaining profiles, indicating that striatal tissue was displaced by implants, but not significantly damaged by them.

Grafting reduces amphetamine-induced rotational asymmetry across all ages

Stereological quantification of THir cell number was used to confirm the absence or presence of a SN lesion in all animals, regardless of age. All lesioned animals exhibited greater than 99% loss of DA neurons in the SN in the lesioned hemisphere (Figure 2, AC). Accordingly, in all age groups, post-lesion amphetamine-induced rotations were >7 ipsilateral rotations per minute over 90 minutes. In sham-grafted rats, the rate of rotational asymmetry was stable over the duration of the study, with no reduction in the number of rotations per minute over time in any age group at 10 weeks post-lesion. In VM grafted rats, there was a significant reduction in the number of amphetamine-induced rotations regardless of host age with the pattern and extent of reduction not differing among groups ($F(2,68)=0.13$, $p>0.05$, Figure 6).

Reversal of levodopa-induced dyskinetic behavior is delayed or absent in aged rats

All parkinsonian rats administered daily levodopa developed LIDs at the same rate and to equal levels across ages prior to grafting (Figure 7). The presence of an intrastriatal VM graft significantly reduced the total LID score across all host age groups in comparison to sham-grafted rats ($F(2,55)=31.32$ $p<0.001$ for treatment effect). However, there were differences in the rate of LID reversal between age groups, with young subjects exhibiting significantly greater improvement at the early post-grafting interval compared to aged grafted subjects (young-grafted vs aged grafted, $p=0.02$; Figure 7 D, E). By 10 weeks post-grafting, this difference disappeared. Expressing the improvement in LID per surviving grafted THir neuron again indicates that middle-aged and aged subjects benefited less (Figure 7F), despite the presence of more grafted cells and graft-derived innervation.

An analysis of individual attributes of dyskinetic behaviors (trunk, neck, forepaw, and hindpaw dystonia; right forepaw dyskinesia (RFPD); and orolingual dyskinesia) revealed

different patterns of graft-associated improvements across age groups (Figure 8). Young grafted rats showed significant recovery at the earliest time point post-grafting (2–4 weeks) for all individual LIDs with the exception of hindpaw dyskinesia ($p<0.05$ for trunk, RFPD, forepaw and orolingual). Middle-aged grafted animals displayed delayed recovery of individual behaviors, but by 6–8 weeks post-grafting exhibited recovery similar to the young grafted subjects. Aged grafted rats showed delayed recovery similar to middle-aged subjects for some LIDs (i.e.: trunk, hindpaw, and orolingual), but by 10 weeks post-grafting most of these benefits disappeared. In addition, aged grafted subjects showed no significant benefit in forepaw dystonia (RFPD) and forepaw dyskinesia over the entire duration of the experiment.

VM grafts reversed elevated FosB/ΔFosB across all ages

As has been previously shown, immunostaining for *FosB/ΔFosB* was increased in the lateral striatum with repeated levodopa treatment that produced LIDs, and remained elevated in sham-grafted rats expressing high levels of LIDs. The presence of an intrastriatal VM graft, in subjects of all age groups, resulted in a significant reduction in *FosB/ΔFosB* staining density compared to sham-grafted rats at 10 weeks post-grafting ($F(2,74)=7.04$, $p=0.002$, Figure 9).

Graft-derived innervation in aging rats make fewer apparent contacts with MSN dendritic spines

Synaptopodin (SP) is an integral protein found in the spine apparatus, an essential component of mature dendritic spines (Vlachos et al., 2009; Segal et al., 2010). We used dual-label immunohistochemistry (TH to label graft-derived DA neurites; SP to label spines of host MSNs) with confocal microscopy to count the number of close appositions, (presumed) synaptic contacts, formed between THir neurites and their preferential target, dendritic spines of host MSNs in young, middle-aged, and aged rats.

The data was expressed as the number of contacts between SP positive puncta per 10 μm of THir neurite. The density of TH-SP contacts was greater for young grafted rats compared to middle-aged and aged grafted rats (young VM grafted: 0.40 ± 0.02 puncta per 10 μm; middle-aged VM grafted: 0.28 ± 0.03 puncta per 10 μm; aged VM grafted: 0.24 ± 0.04 puncta per 10 μm, $F(2,15)=5.14$, $p=0.02$, young vs middle-aged and young vs aged, $p<0.05$, Figure 10A). Moreover, the SP contact density per surviving grafted dopaminergic neuron was greater for young grafted rats compared to middle aged and aged grafted rats (young VM grafted: 0.00040 ± 0.00010 puncta per 10 μm; middle-aged VM grafted: 0.00010 ± 0.00002 puncta per 10 μm; aged VM grafted: 0.00004 ± 0.00001 puncta per 10 μm, $F(2,14)=11.73$, $p<0.002$, post-hoc young vs middle and young vs aged $p<0.05$, Figure 10B). Finally, the SP contact density per percent reduction in LID severity post grafting was greater for young grafted rats compared to middle aged and aged grafted rats (young VM grafted: 0.0060 ± 0.0008 puncta per 10 μm; middle-aged VM grafted: 0.0040 ± 0.0005 puncta per 10 μm; aged VM grafted: 0.0040 ± 0.0010 puncta per 10 μm, $F(2,14)=5.21$, $p=0.02$, young vs middle-aged and young vs aged, $p<0.05$, Figure 10C).

Discussion

Our results indicate that obvious differences in DA graft characteristics previously observed in the aged brain can be adequately resolved. Specifically, upward adjustment of the number of cells intended to replace striatal DA resulted in increased survival, reinnervation and reversal of amphetamine-induced rotational behavior. However, when the analysis included additional levels of complexity, differences associated with the aging environment persisted. While DA grafts in aging subjects yield improvement in LID, and reversed a signature increase in immediate early gene expression associated with LID (i.e.: FosB), correction of these behaviors comparable to grafted young subjects was delayed or absent. Of significant note, the delay or absence of functional benefit occurred despite nearly 5-fold more THir neurons in, and up to 2-fold greater fiber density derived from the grafts of aged subjects compared to young. One structural correlate of this difference was a significant decline in evidence of contacts between graft-derived innervation and their striatal target, MSNs, in the aging environment, suggestive of a decrease in anatomical integration of graft and host. It is likely that this apparent inability to fully integrate with the host brain is a significant limitation for the prospects of nerve terminal replacement therapies in aged individuals. Our previous work has shown that even in the young host when synapses are established between grafted DA neurons and MSNs the location and ultrastructural morphology of these contacts is altered by the remodeling that occurs in the DA-depleted striatum (Soderstrom et al., 2008).

While the additional impact of aging on DA-terminal remodeling remains to be fully investigated, the current study suggests that dendritic spine pathology may play a role in the age-related reduction in graft efficacy. Specifically, in the DA-depleted, parkinsonian striatum there is a loss of dendritic spines on MSNs (McNeil et al., 1988; Day et al., 2006; Soderstrom et al., 2010). In the normal striatum, dendritic spines are critical structural elements where DA terminals predominantly synapse onto the neck of the spine modulating afferent glutamatergic input that synapses predominantly onto the heads of the same spines (for review, Soderstrom et al., 2008). In the DA-depleted striatum where spine loss occurs, grafted DA neurons establish new synapses with the dendritic shaft of MSNs more frequently than the spines (Freund et al., 1985; Mahalik et al., 1985; Clarke et al., 1988; Leranth et al., 1998; Soderstrom et al., 2008). Indeed, the preservation of striatal dendritic spines in the presence of severe DA depletion significantly enhances the functional efficacy of grafted DA neurons in young parkinsonian rats (Soderstrom et al., 2010). Our current data indicate that the SP-TH contact density is associated with the degree of reduction in LID severity post grafting and that this was greater for young grafted rats compared to middle aged and aged grafted rats. Spine loss in the aged brain has been extensively studied in regions such as the hippocampus and neocortex, however significantly less is known about age-related dendritic spine changes in the striatum (for review, Dickstein et al., 2013). While a decrease in dendritic spine density in the striatum (caudate) of cats (Levine et al., 1986) and a loss of striatal axospinous synapses (Itzev et al, 2001, 2003) have been reported, the impact of age on striatal spine density in the rat remains to be fully characterized. While the brains in the current study were not prepared to be compatible with Golgi impregnation (Levine et al., 2013) and spine quantification, as part of a separate study, we have recently

found using Golgi impregnation methods in parkinsonian Sprague Dawley rats that there is a significant 15% decrease in striatal spine density in young (3 months) versus aged (20 months) subjects (unpublished observation); a finding consistent with age-related spine loss in other brain regions (e.g.: Dickstein et al., 2013). Only a subset of dendritic spines express SP and the spine apparatus to which SP is integrally associated (Vlachos et al., 2009). In these spines, SP has been demonstrated to be critically involved with spine calcium store-associated induction of long-term plasticity involving glutamate receptors and long-term potentiation (Vlachos et al., 2009; Segal et al., 2010). While our SP data does not allow for assessment of spine density *per se*, it does support the view that alterations in striatal dendritic spine-associated plasticity in the aged host may be linked to deficits in graft efficacy.

Neuroinflammation is a prominent feature of normal brain aging and is linked to age-related synaptic dysfunction (for review see Sama and Norris 2013). The scope of the present project did not allow direct examination of the contribution of this variable to the effects observed. However, some impact is likely as in addition to aging, increased inflammation is associated with DA-depletion and cell transplantation (e.g.: Kordower et al., 1997; Bakay et al., 1998; Soderstrom et al., 2008; Barnum and Tansey 2010). Indeed, our previous work indicates that activation of the immune system can have profound effects on the pattern and ultrastructure of graft-derived synaptic contacts (Soderstrom et al., 2008). Thus, the challenge of re-building new, normal synaptic circuits with grafted DA neurons may be untenable without appropriate modulation/supplementation of the environment through the use of adjunct therapeutic interventions directed at mitigating glial activation and calcium dysregulation.

Given that grafting paradigms in PD patients are usually reserved for individuals in greatest need of treatment, those with advanced disease, severe DA depletion, and often in patients of advanced years, optimizing the use of cell transplants in aged individuals is of significant clinical value and interest. Previous studies in animal models of aging and PD identify some of the challenges facing this task; specifically, decreased trophic support (Ling et al., 2000) and decreased compensatory mechanisms in response to DA-depletion (Collier et al., 2007). The results of the current study demonstrate that even when a large number of DA neurons are shown to survive in the aged parkinsonian rat brain, the behavioral impact is delayed and inferior on a per cell basis to that seen with significantly fewer neurons in younger subjects.

Conclusions

As PD diagnostic techniques become further refined and therapeutic options are optimized, the legitimacy of early disease intervention is becoming increasingly realistic. Age remains the greatest risk factor for PD, and early intervention will likely offer the most promising therapeutic option for patients. Results from this study offer additional evidence that therapeutic efficacy of DA terminal replacement diminishes with age, supporting the rationale of earlier intervention.

Cell replacement as a therapy for PD is widely considered passé. Yet, the rationale for providing a cell of appropriate biology as a source of chemical and structural repair of the

damaged DA system remains compelling. While accurate identification of the “right patient at the right time” remains ill-defined, there are clear examples of the enduring benefits of cell transplantation (Kefalopoulou et al., 2014; Hallett et al., 2014). Increased awareness that the earliest event in DA system degeneration in PD is loss of striatal innervation (Kordower et al., 2013), and consequent aberrant therapy-resistant remodeling of the striatum (Steece-Collier et al., 2012; Zhang et al., 2013), provides additional conceptual support for interventions that subvert denervation as cell transplantation has the capacity to do (Abbott, 2014).

Acknowledgments

The authors would like to acknowledge Nathan D. Levine and Brian F. Daley for their technical and surgical expertise.

Support

This work was supported by NIH Grants R01 NS04513 (K.S.-C.), P50 NS058830 (T.J.C., K.S.-C., C.E.S.) and the Edwin A. Brophy endowment at Michigan State University (TJC).

References

Abbott A. Fetal-cell revival for Parkinson’s. Nature. 2014; 510:195–196. [PubMed: 24919900]

Ambasudhan R, Dolatabadi N, Nutter A, Masliah E, Mckercher SR, Lipton SA. Potential for cell therapy in Parkinson’s disease using genetically programmed human embryonic stem cell-derived neural progenitor cells. J Comp. Neurol. 2014; 522:2845–2856. [PubMed: 24756727]

Andersson M, Hibertson A, Cenci MA. Striatal fosB expression is causally linked with l-DOPA-induced abnormal involuntary movements and the associated upregulation of striatal prodynorphin mRNA in a rat model of Parkinson’s disease. Neurobiol. Dis. 1999; 6:461–474. [PubMed: 10600402]

Andersson M, Westin JE, Cenci MA. Time course of striatal DeltaFosB-like immunoreactivity and prodynorphin mRNA levels after discontinuation of chronic dopaminomimetic treatment. Eur. J. Neurosci. 2003; 17:661–666. [PubMed: 12581184]

Annett LE, Torres EM, Clarke DJ, Ishida Y, Barker RA, Ridley RM, Baker HF, Dunnett SB. Survival of nigral grafts within the striatum of marmosets with 6-OHDA lesions depends critically on donor embryo age. Cell Transplant. 1997; 6:557–569. [PubMed: 9440865]

Arjona V, Mínguez-Castellanos A, Montoro RJ, Ortega A, Escamilla F, Toledo-Aral JJ, Pardal R, Méndez-Ferrer S, Martín JM, Pérez M, Katati MJ, Valencia E, García T, López-Barneo J. Autotransplantation of human carotid body cell aggregates for treatment of Parkinson’s disease. Neurosurgery. 2003; 53:321–328. [PubMed: 12925247]

Bakay RA, Boyer KL, Freed CR, Ansari AA. Immunological responses to injury and grafting in the central nervous system of nonhuman primates. Cell Transplant. 1998; 7:109–120. [PubMed: 9588593]

Barnum CJ, Tansey MG. Modeling neuroinflammatory pathogenesis of Parkinson’s disease. Prog Brain Res. 2010; 184:113–132. [PubMed: 20887872]

Borlongan CV, Zhou FC, Hayashi T, Su TP, Hoffer BJ, Wang Y. Involvement of GDNF in neuronal protection against 6-OHDA-induced parkinsonism following intracerebral transplantation of fetal kidney tissues in adult rats. Neurobiol. Dis. 2001; 8:636–646. [PubMed: 11493028]

Breysse N, Carlsson T, Winkler C, Björklund A, Kirik D. The functional impact of the intrastriatal dopamine neuron grafts in parkinsonian rats is reduced with advancing disease. J. Neurosci. 2007; 27:5849–5856. [PubMed: 17537955]

Buttery PC, Barker RA. Treating Parkinson’s disease in the 21st century: can stem cell transplantation compete? J. Comp. Neurol. 2014; 522:2802–2816. [PubMed: 24610597]

Cahill DW, Olanow CW. Autologous adrenal medulla to caudate nucleus transplantation in advanced Parkinson's disease: 18 month results. Prog. Brain Res. 1990; 82:637–642. [PubMed: 2290965]

Clarke DJ, Brundin P, Strecker RE, Nilsson OG, Bjorklund A, Lindvall O. Human fetal dopamine neurons grafted in a rat model of Parkinson's disease: ultrastructural evidence for synapse formation using tyrosine hydroxylase immunocytochemistry. Exp. Brain Res. 1988; 73:115–126. [PubMed: 3145209]

Collier TJ, Dung Ling Z, Carvey PM, Fletcher-Turner A, Yurek DM, Sladek JR Jr, Kordower JH. Striatal trophic factor activity in aging monkeys with unilateral MPTP-induced parkinsonism. Exp. Neurol. 2005; 191:S60–S70. [PubMed: 15629762]

Collier TJ, Lipton J, Daley BF, Palfi S, Chu Y, Sortwell C, Bakay RA, Sladek JR Jr, Kordower JH. Aging-related changes in the nigrostriatal dopamine system and the response to MPTP in nonhuman primates: diminished compensatory mechanisms as a prelude to parkinsonism. Neurobiol. Dis. 2007; 26:56–65. [PubMed: 17254792]

Collier TJ, Sortwell CE, Dayley BF. Diminished viability, growth, and behavioral efficacy of fetal dopamine neuron grafts in aging rats with long-term dopamine depletion: an argument for neurotrophic supplementation. J. Neurosci. 1999; 19:5563–5573. [PubMed: 10377363]

Croll SD, Ip NY, Lindsay RM, Wiegand SJ. Expression of BDNF and trkB as a function of age and cognitive performance. Brain Res. 1998; 812:200–208. [PubMed: 9813325]

Dickstein DL, Weaver CM, Luebke JI, Hof PR. Dendritic spine changes associated with normal aging. Neuroscience. 2013; 251:21–32. [PubMed: 23069756]

Evans JR, Mason SL, Barker RA. Current status of clinical trials of neural transplantation in Parkinson's disease. Prog. Brain Res. 2012; 200:169–198. [PubMed: 23195419]

Ferrari D, Sanchez-Pernaute R, Lee H, Studer L, Isacson O. Transplanted dopamine neurons derived from primate ES cells preferentially innervate DARPP-32 striatal progenitors within the graft. Eur. J. Neurosci. 2006; 24:1885–1896. [PubMed: 17067292]

Freund TF, Bolam JP, Bjorklund A, Stenevi U, Dunnett SB, Powell JF, Smith AD. Efferent synaptic connections of grafted dopaminergic neurons reinnervating the host neostriatum: a tyrosine hydroxylase immunocytochemical study. J. Neurosci. 1985; 5:603–616. [PubMed: 2857778]

Fitoussi N, Sotnik-Barkai I, Tornatore C, Herzberg U, Yadid G. Dopamine turnover and metabolism in the striatum of parkinsonian rats grafted with genetically-modified human astrocytes. Neuroscience. 1998; 85:405–413. [PubMed: 9622240]

Freed CR, Greene PE, Breeze RE, Tsai WY, DuMouchel W, Kao R, Dillon S, Winfield H, Culver S, Trajanowski JQ, Eidelberg D, Fahn S. Transplantation of embryonic dopamine neurons for severe Parkinson's disease. N. Engl. J. Med. 344:710–719. [PubMed: 11236774]

Freed CR, Leehey MA, Zawada M, Bjugstad K, Thompson L, Breeze RE. Do patients with Parkinson's disease benefit from embryonic dopamine cell transplantation? J. Neurol. 2003; 250:III44–III46. [PubMed: 14579124]

Freeman TB, Olanow GW. Fetal homotransplants in the treatment of Parkinson's disease. Arch. Neurol. 1991; 48:900–902. [PubMed: 1953410]

Freeman TB, Olanow CW, Hauser RA, Nauert GM, Smith DA, Borlongan CV, Sanberg PR, Holt DA, Kordower JH, Vingerhoets FJ, et al. Bilateral fetal nigral transplantation into the postcommissural putamen in Parkinson's disease. Ann. Neurol. 1995; 38:379–388. [PubMed: 7668823]

Freeman TB, Sanberg PR, Nauert GM, Boss BD, Spector D, Olanow CW, Kordower JH. The influence of donor age on the survival of solid and suspension intraparenchymal human embryonic nigral grafts. Cell Transplant. 1995; 4:141–154. [PubMed: 7728329]

Goetz CG, Olanow CW, Koller WC, Penn RD, Cahill D, Morantz R, Stebbins G, Tanner CM, Klawans HL, Shannon KM. Multicenter study of autologous adrenal medullary transplantation to the corpus striatum in patients with advanced Parkinson's disease. N. Engl. J. Med. 1989; 320:337–341. [PubMed: 2643770]

Goren B, Kahveci N, Eyigor O, Alkan T, Korfali E, Ozluk K. Effects of intranigral vs intrastriatal fetal mesencephalic neural grafts on motor behavior disorders in a rat Parkinson model. Surg. Neurol. 2005; 64:S33–S41. [PubMed: 16256839]

Gundersen HJ, Bagger P, Bendtsen TF, Evans SM, Korbo L, Marcussen N, Møller A, Nielsen K, Nyengaard JR, Pakkenberg B, et al. The new stereological tools: disector, fractionator, nucleator

and point sampled intercepts and their use in pathological research and diagnosis. APMIS. 1988; 96:857–881. [PubMed: 3056461]

Gundersen HJ, Bendtsen TF, Korbo L, Marcussen N, Møller A, Nielsen K, Nyengaard JR, Pakkenberg B, Sørensen FB, et al. Some new, simple and efficient stereological methods and their use in pathological research and diagnosis. APMIS. 1988; 96:379–394. [PubMed: 3288247]

Hagell P, Cenci MA. Dyskinesias and dopamine cell replacement in Parkinson's disease: a clinical perspective. Brain Res. Bull. 2005; 68:4–15. [PubMed: 16324999]

Hagell P, Piccini P, Björklund A, Brundin P, Rehncrona S, Widner H, Crabb L, Pavese N, Oertel WH, Quinn N, Brooks DJ, Lindvall O. Dyskinesias following neural transplant in Parkinson's disease. Nat. Neurosci. 2002; 5:627–628. [PubMed: 12042822]

Hallett PJ, Cooper O, Sadi D, Robertson H, Mendez I, Isacson O. Long-term health of dopaminergic neuron transplants in Parkinson's disease patients. Cell Reports. 2014; 7:1755–1761. [PubMed: 24910427]

Hands S, Sinadinos C, Wyttenbach A. Polyglutamine gene function and dysfunction in the ageing brain. Biochim. Biophys. Acta. 2008; 1779:507–521. [PubMed: 18582603]

Hickey P, Stacy M. AAV2-neurturin (CERE-120) for Parkinson's disease. Expert Opin. Biol. Ther. 2013; 13:137–145. [PubMed: 23228025]

Itzev D, Lolova I, Lolov S, Usunoff KG. Age-related changes in the synapses of the rat's neostriatum. Arch Physiol Biochem. 2001; 109:80–89. [PubMed: 11471075]

Itzev DE, Lolov SR, Usunoff KG. Aging and synaptic changes in the paraventricular hypothalamic nucleus of the rat. Acta Physiol Pharmacol Bulg. 2003; 27:75–82. [PubMed: 14570152]

Kanaan NM, Kordower JH, Collier TJ. Age-related changes of Marinesco bodies and lipofuscin in rhesus monkey midbrain dopamine neurons: relevance to selective neuronal vulnerability. J. Comp. Neurol. 2008; 502:683–700. [PubMed: 17436290]

Kanaan NM, Kordower JH, Collier TJ. Age and region-specific responses of microglia, but not astrocytes, suggest a role in selective vulnerability of dopamine neurons after 1-methyl-4-phenyl-1,2,3,6-tetrahydropyridine exposure in monkeys. Glia. 2008; 56:1199–1214. [PubMed: 18484101]

Kefalopoulou Z, Aviles-Olmos I, Foltynie T. Critical aspects of clinical trial design for novel cell and gene therapies. Parkinsons Dis. 2011; 2011:804041. (?). [PubMed: 22254150]

Kefalopoulou Z, Politis M, Piccini P, Mencacci N, Bhatia K, Jahanshahi M, Widner H, Rehncrona S, Brundin P, Bjorklund A, Lindvall O, Limousin P, Quinn N, Foltynie T. Long-term clinical outcome of fetal cell transplantation for Parkinson disease: two case reports. JAMA Neurol. 2014; 71:83–87. [PubMed: 24217017]

Kordower JH, Bjorklund A. Trophic factor gene therapy for Parkinson's disease. Mov. Disord. 2013; 28:96–109. [PubMed: 23390096]

Kordower JH, Chu Y, Stebbins GT, DeKosky ST, Cochran EJ, Bennett D, Mufson EJ. Loss and atrophy of layer II entorhinal cortex neurons in elderly people with mild cognitive impairment. Ann. Neuol. 2001; 49:202–213.

Kordower JH, Freeman TB, Bakay RA, Goetz CG, Olanow CW. Treatment with fetal allografts. Neurology. 1997; 48:1137–1138.

Kordower JH, Freeman TB, Chen EY, Mufson EJ, Sanberg PR, Hauser RA, Snow B, Olanow CW. Fetal nigral grafts survive and mediate clinical benefit in a patient with Parkinson's disease. Mov. Disord. 1998; 13:383–393. [PubMed: 9613726]

Kordower JH, Freeman TB, Snow BJ, Vingerhoets FJ, Mufson EJ, Sandberg PR, Hauser RA, Smith DA, Nauert GM, Perl DP, et al. Neuropathological evidence of graft survival and striatal reinnervation after the transplantation of fetal mesencephalic tissue in a patient with Parkinson's disease. N. Engl. J. Med. 1995; 332:1118–1124. [PubMed: 7700284]

Kordower JH, Olanow CW, Dodiya HB, Chu Y, Beach TG, Adler CH, Halliday GM, Bartus RT. Disease duration and the integrity of the nigrostriatal system in Parkinson's disease. Brain. 2013; 136:2419–2431. [PubMed: 23884810]

Kordower JH, Styren S, Clarke M, DeKosky ST, Olanow CW, Freeman TB. Fetal grafting for Parkinson's disease: expression of immune markers in two patients with functioning fetal nigral implants. Cell Transplant. 1997; 6:213–219. [PubMed: 9171154]

Larsen M, Bjarkam CR, Østergaard K, West MJ, Sørensen JC. The anatomy of the porcine subthalamic nucleus evaluated with immunohistochemistry and design-based stereology. Anat. Embryol. (Berl.). 2004; 208:239–247. [PubMed: 15168115]

Lee CS, Cenci MA, Schulzer M, Björklund A. Embryonic ventral mesencephalic grafts improve levodopa-induced dyskinesia in a rat model of Parkinson's disease. Brain. 2000; 123:1365–1379. [PubMed: 10869049]

Lee CK, Weindruch R, Prolla TA. Gene-expression profile of the ageing brain in mice. Nat Genet. 2000; 25:294–297. [PubMed: 10888876]

Leranth C, Sladek JR Jr, Roth RH, Redmond DE Jr. Efferent synaptic connections of dopaminergic neurons grafted into the caudate nucleus of experimentally induced parkinsonian monkeys are different from those of control animals. Exp. Brain Res. 1998; 123:323–333. [PubMed: 9860271]

Levine MS, Adinolfi AM, Fisher RS, Hull CD, Buchwald NA, McAllister JP. Quantitative morphology of medium-sized caudate spiny neurons in aged cats. Neurobiol Aging. 1986; 7:277–286. [PubMed: 3748270]

Levine ND, Rademacher DJ, Collier TJ, O'Malley JA, Kells AP, San Sebastian W, Bankiewicz KS, Steece-Collier K. Advances in thin tissue Golgi-Cox impregnation: fast, reliable methods for multi-assay analyses in rodent and non-human primate brain. J Neurosci Methods. 2013; 213(2): 214–227. [PubMed: 23313849]

Ling ZD, Collier TJ, Sortwell CE, Lipton JW, Vu TQ, Robie HC, Carvie PM. Striatal trophic activity is reduced in the aged rat brain. Brain Res. 2000; 856:301–309. [PubMed: 10677639]

Ma Y, Peng S, Dhawan V, Eidelberg D. Dopamine cell transplantation in Parkinson's disease: challenge and perspective. Br. Med. Bull. 2011; 100:173–189. [PubMed: 21875864]

Mahalik TJ, Finger TE, Stromberg I, Olson L. Substantia nigra transplants into denervated striatum of the rat: ultrastructure of graft and host interconnections. J. Comp. Neurol. 1985; 240:60–70. [PubMed: 2865279]

Maries E, Kordower JH, Chu Y, Collier TJ, Sortwell CE, Olaru E, Shannon K, Steece-Collier K. Focal but not widespread grafts induce novel dyskinetic behavior in parkinsonian rats. Neurobiol. Dis. 2006; 21:165–180. [PubMed: 16095907]

Matarredona ER, Meyer M, Seiler RW, Widmer HR. CGP 3466 increases survival of cultured fetal dopaminergic neurons. Restor. Neurol. Neurosci. 2003; 21:19–37. [PubMed: 12808199]

Murray CA, Lynch MA. Evidence that increased hippocampal expression ofthe cytokine interleukin-1 beta is a common trigger for age- and stress-inducedimpairments in long-term potentiation. J. Neurosci. 1998; 18:2974–2981. [PubMed: 9526014]

Olanow CW, Freeman T, Kordower J. Transplantation of embryonic dopamine neurons for severe Parkinson's disease. N. Engl. J. Med. 2001; 345:146. author reply 147. [PubMed: 11450669]

Olanow CW, Koller W, Goetz CG, Stebbins GT, Cahill DW, Gauger LL, Morantz R, Penn RD, Tanner CM, Klawans HL, et al. Autologous transplantation of adrenal medulla in Parkinson's disease. 18-month results. Arch. Neurol. 1990; 47:1286–1289. [PubMed: 2252446]

Olanow CW, Kordower JH, Freeman TB. Fetal nigral transplantation as a therapy for Parkinson's disease. Trends Neurosci. 1996; 19:102–109. [PubMed: 9054056]

Ouimet CC, Langley-Gullion KC, Greengard P. Quantitative immunocytochemistry of DARPP-32-expressing neurons in the rat caudoatoputamen. Brain Res. 1998; 808:8–12. [PubMed: 9795103]

Paxinos, G.; Watson, C. The Rat Brain in Stereotaxic Coordinates. Academic Press; New York: 1998.

Picconi B, Centonze D, Håkansson K, Bernardi G, Greengard P, Fisone G, Cenci MA, Calabresi P. Loss of bidirectional synaptic plasticity in L-DOPA-induced dyskinesia. Nat. Neurosci. 2003; 6:501–506. [PubMed: 12665799]

Piccini P, Pavese N, Hagell P, Reimer J, Björklund A, Oertel WH, Quinn NP, Brooks DJ, Lindvall O. Factors affecting the clinical outcome after neural transplantation in Parkinson's disease. Brain. 2005; 128:2977–2986. [PubMed: 16246865]

Picconi B, Pisani A, Barone I, Bonsi P, Centonze D, Bernardi G, Calabresi P. Pathological synaptic plasticity in the striatum: implications for Parkinson's disease. Neurotoxicology. 2005; 26:779–783. [PubMed: 15927256]

Pisani A, Centonze D, Bernardi G, Calabresi P. Striatal synaptic plasticity: implications for motor learning and Parkinson's disease. Mov. Disord. 2005; 20:395–402. [PubMed: 15719415]

Sable V, Sailaja K, Gopinath G, Tandon PN. Fetal dopaminergic neurons transplanted to the normal striatum of neonatal or adult rats and to the denervated striatum of adult rats. J. Neural Transplant. Plast. 1997; 6:73–81. [PubMed: 9306239]

Sama DM, Norris CM. Calcium dysregulation and neuroinflammation: discrete and integrated mechanisms for age-related synaptic dysfunction. Ageing Res Rev. 2013; 12:982–995. [PubMed: 23751484]

Santini E, Valjent E, Usiello A, Carta M, Borgkvist A, Girault JA, Hervé D, Greengard P, Fisone G. Critical involvement of cAMP/DARPP-32 and extracellular signal-regulated protein kinase signaling in L-DOPA-induced dyskinesia. J. Neurosci. 2007; 27:6995–7005. [PubMed: 17596448]

Segal M, Vlachos A, Korkotian E. The spine apparatus, synaptopodin, and dendritic spine plasticity. Neuroscientist. 2010 Apr; 16(2):125–131. [PubMed: 20400711]

Sladek JR Jr, Collier TJ, Elsworth JD, Roth RH, Taylor JR, Redmond DE Jr. Intrastriatal grafts from multiple donors do not result in a proportional increase in survival of dopamine neurons in nonhuman primates. Cell Transplant. 1998; 7:87–96. [PubMed: 9588591]

Soderstrom KE, Meredith G, Freeman TB, McGuire SO, Collier TJ, Sortwell CE, Wu Q, Steece-Collier K. The synaptic impact of the host immune response in a parkinsonian allograft rat model: Influence on graft-derived aberrant behaviors. Neurobiol. Dis. 2008; 32:229–242. [PubMed: 18672063]

Sortwell CE, Camargo MD, Pitzer MR, Gyawali S, Collier TJ. Diminished survival of mesencephalic dopamine neurons grafted into aged hosts occurs during the immediate postgrafting interval. Exp Neurol. 2001; 169(1):23–29. [PubMed: 11312554]

Steece-Collier K, Collier TJ, Danielson PD, Kurlan R, Yurek DM, Sladek JR Jr. Embryonic mesencephalic grafts increase levodopa-induced forelimb hyperkinesia in parkinsonian rats. Mov. Disord. 2003; 18:1442–1454. [PubMed: 14673880]

Steece-Collier K, Collier TJ, Sladek JR Jr. Chronic levodopa impairs morphological development of grafted embryonic dopamine neurons. Exp. Neurol. 1990; 110:201–208. [PubMed: 2226699]

Steece-Collier K, Yurek DM, Collier TJ, Junn FS, Sladek JR Jr. The detrimental effect of levodopa on behavioral efficacy of fetal dopamine neuron grafts in rats is reversible following prolonged withdrawal of chronic dosing. Brain Res. 1995; 676:404–408. [PubMed: 7614013]

Steece-Collier K, Rademacher DJ, Soderstrom K. Anatomy of graft-induced dyskinesias: circuit remodeling in the parkinsonian striatum. Basal Ganglia. 2012; 2:15–30. [PubMed: 22712056]

Strömberg I, Bygdeman M, Goldstein M, Seiger A, Olson L. Human fetal substantia nigra grafted to the dopamine-denervated striatum of immunosuppressed rats: evidence for functional reinnervation. Neurosci. Lett. 1986; 71:271–276. [PubMed: 2879264]

Sundberg M, Isacson O. Advances in stem cell-generated transplantation therapy for Parkinson's disease. Expert Opin. Biol. Ther. 2014; 14:437–453. [PubMed: 24437368]

Terpstra BT, Collier TJ, Marchionini DM, Levine ND, Paumier KL, Sortwell CE. Increased cell suspension concentration augments the survival rate of grafted tyrosine hydroxylase immunoreactive neurons. J Neurosci Methods. 2007; 166:13–19. [PubMed: 17706789]

Thompson VB, Koprich JB, Chen EY, Kordower JH, Terpstra BT, Lipton JW. Prenatal exposure to MDMA alters noradrenergic neurodevelopment in the rat. Neurotoxicol. Teratol. 2012; 34:206–213. [PubMed: 21978916]

Toledo-Aral JJ, Méndez-Ferrer S, Pardal R, Echevarría M, López-Barneo J. Trophic restoration of the nigrostriatal dopaminergic pathway in long-term carotid body-grafted parkinsonian rats. J. Neurosci. 2003; 23:141–148. [PubMed: 12514210]

Torres, EM.; Monville, C.; Gates, MA.; Bagga, V.; Dunnett, SB. Improved survival of young donor age dopamine grafts in a rat model of Parkinson's disease. Vol. 146. 2007; p. 1606-1617.

Yoshizaki T, Inaji M, Kouike H, Shimazaki T, Sawamoto K, Ando K, Date I, Kobayashi K, Suhura T, Uchiyama Y, Okana H. Isolation and transplantation of dopaminergic neurons generated from mouse embryonic stem cells. Neurosci. Lett. 2004; 363:33–37. [PubMed: 15157991]

Vlachos A, Korkotian E, Schonfeld E, Copanaki E, Deller T, Segal M. Synaptopodin regulates plasticity of dendritic spines in hippocampal neurons. J Neurosci. 2009; 29(4):1017–1033. [PubMed: 19176811]

Winkler C, Georgievska B, Carlsson T, Lacar B, Kirik D. Continuous exposure to glial cell line-derived neurotrophic factor to mature dopaminergic transplants impairs the graft's ability to improve spontaneous motor behavior in parkinsonian rats. Neuroscience. 2006; 141:521–531. [PubMed: 16697115]

Zhang Y, Meredith GE, Mendoza-Elias N, Rademacher DJ, Tseng KY, Steece-Collier K. Aberrant restoration of spines and their synapses in L-DOPA-induced dyskinesia: involvement of corticostriatal but not thalamostriatal synapses. J. Neurosci. 2013; 33:11655–11667. [PubMed: 23843533]

Highlights

- Dopamine neurons were grafted into young, middle and aged parkinsonian rats.
- Two-fold and 5-fold more cells were grafted into middle and aged rats than young.
- Robust graft survival and neurite outgrowth was observed in aged rats.
- Behavioral benefit was inferior in aged rats compared to younger rats.
- Age-related dendritic spine pathology may underlie suboptimal functional benefit.

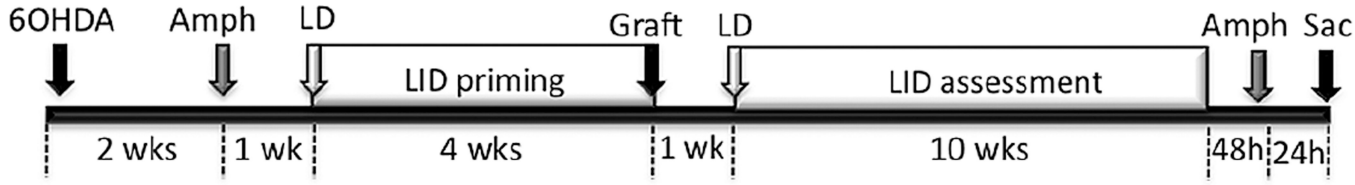

Figure 1.

Time course of surgical procedures, behavioral evaluation, and drug treatments. Rats were rendered parkinsonian with 6-OHDA. Two weeks after 6OHDA, amphetamine-induced rotational behavior was evaluated to confirm lesion status. Three weeks after 6OHDA parkinsonian rats were primed with daily (M-Fr) levodopa or saline for 4 weeks prior to grafting. Once stable dyskinesias were established following levodopa priming, ventral mesencephalic or sham grafts were implanted into the parkinsonian striatum. Levodopa and vehicle injections were withdrawn for 1 week following graft surgery, after which time daily injections were continued for 10 weeks. Levodopa was withdrawn for 48 hours prior to a second amphetamine-induced rotational behavioral evaluation used to assess graft efficacy. Twenty-four hours after the last amphetamine test, rats were humanely sacrificed.
Abbreviations: 6-OHDA= 6-hydroxydopamine; Amph= amphetamine; LD= levodopa; LID=levodopa-induced dyskinesia; Sac= sacrifice.

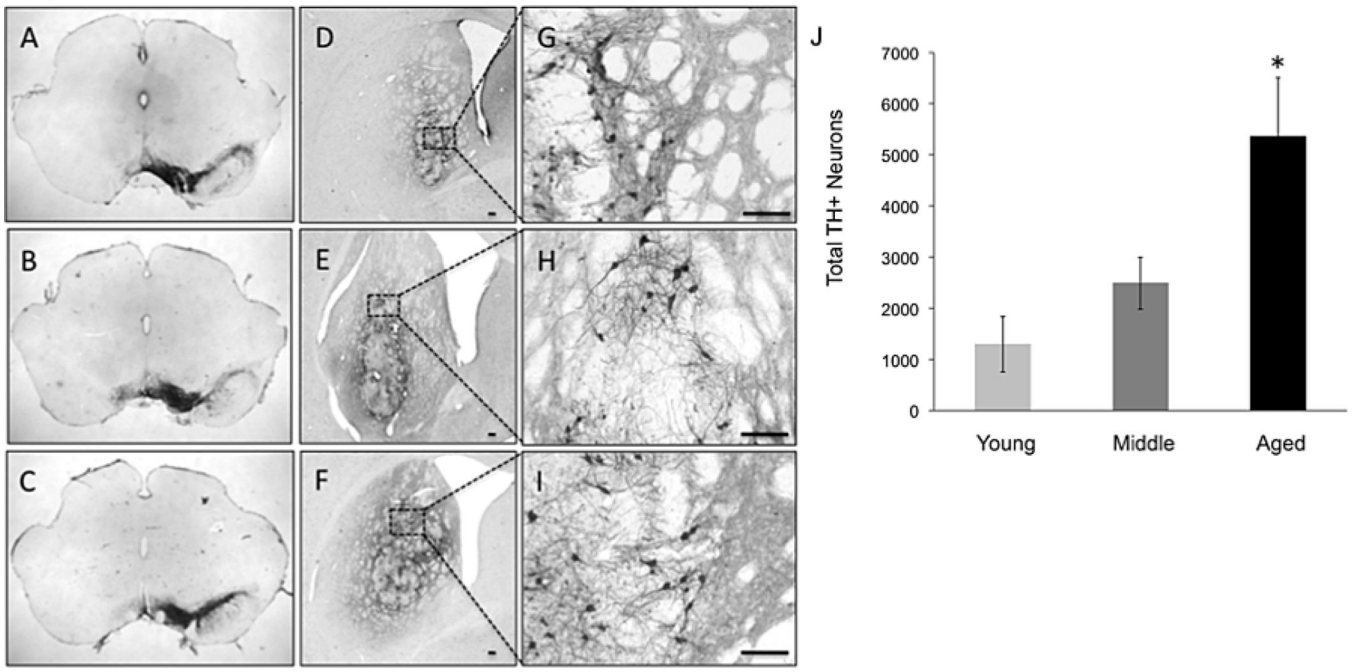

Figure 2.

Micrographs of TH+ nigral neurons (**A-C**) and grafted neurons in young (**D, G**), middle-aged (**E, H**), and aged (**F, I**) rats. 6-OHDA-mediated nigral DA neuron loss is near complete across all ages (**A-C**). High magnification (100X) view of the graft and its medial border of the graft in young (**D**), middle-aged (**E**), and aged (**F**) VM grafted rat. Low magnification (4X) view of the VM graft in the striatum of young (**G**), middle-aged (**H**), and aged (**I**) VM grafted rats. (**J**) Aged rats have significantly greater numbers of surviving TH+ neurons in the grafted striatum compared to middle-aged and young VM grafted rats as denoted by the asterisk ($p < 0.05$). Scale bars represent 100 um.

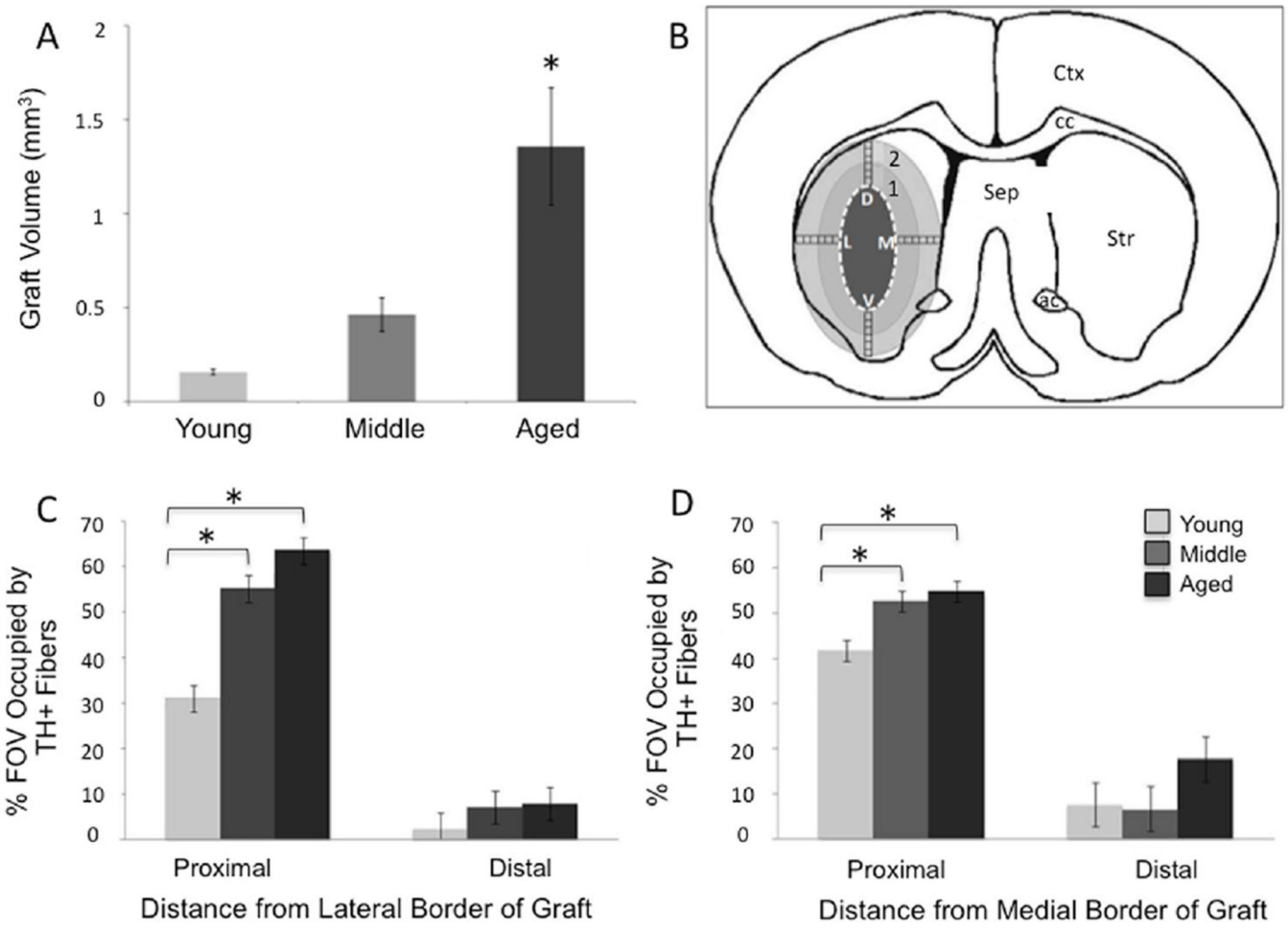

Figure 3.

Graft volume and neurite outgrowth. **A)** The volume of the VM graft in aged rats was significantly greater than in middle-aged or young VM grafted rats. The asterisk denotes significant difference of aged versus young and middle-aged groups at $p < 0.05$. **B)** Neurite density analysis was performed in 6 consecutive fields of view (boxes) at 40X from the dorsal (D) and medial (M) ventral (V) and lateral (L) borders of the graft. The '1' denotes proximal fields of view and the '2' denotes distal fields of view. Abbreviations: ac, anterior commissure; cc, corpus collosum; Sep, septum; STR, striatum; Ctx, cortex. **C, D)** Percent of the field of view (FOV) occupied with TH+ neurites lateral (C) and medial (D) to the center of the graft. The asterisks denote significant differences ($p < 0.05$) for indicated comparison. Proximal: 0–850μm from the graft border; Distal: 850–1700μm from the graft border.

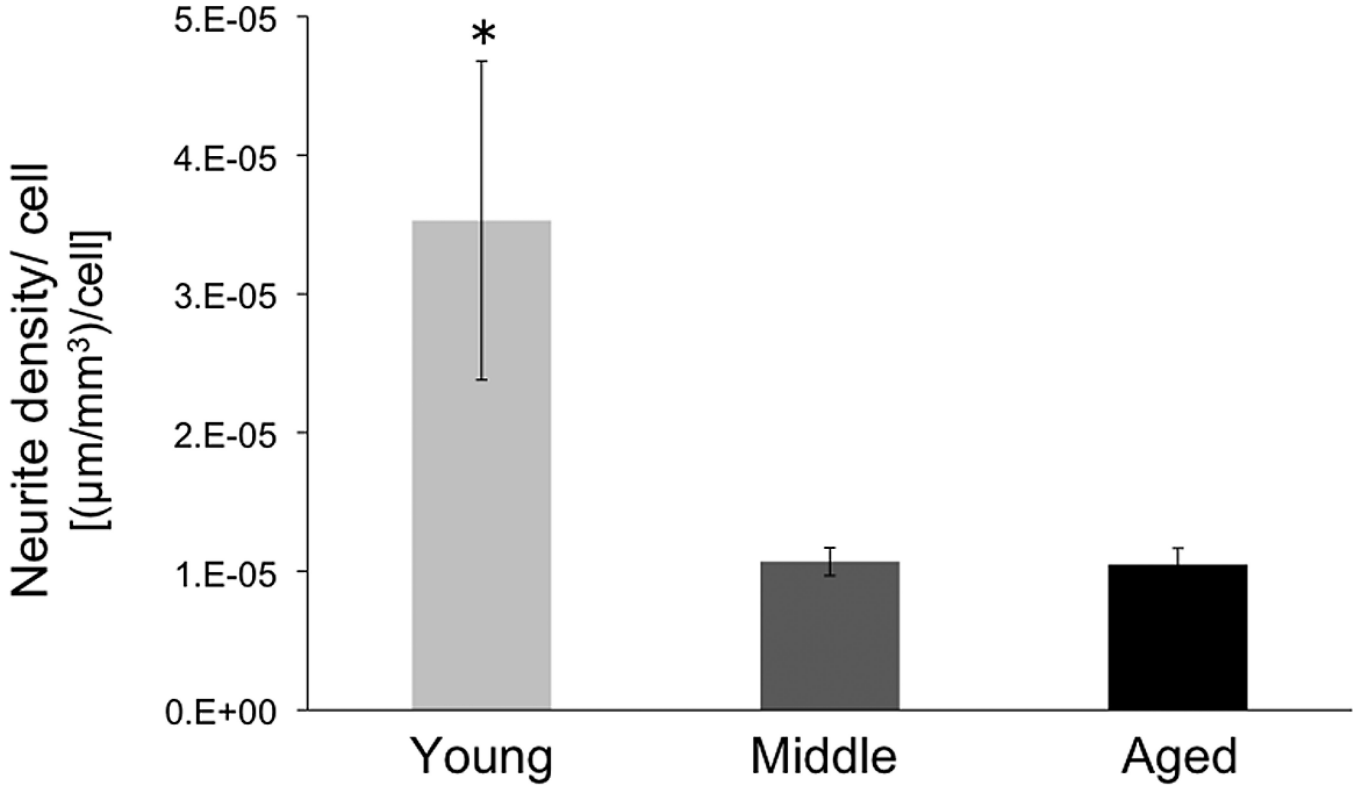

Figure 4.

Neurite density per grafted TH+ cell. Neurite density lateral to the graft was quantified with the Space Balls stereology probe (Microbrightfield) in young, middle-aged, and aged VM grafted rats and adjusted to the number of surviving TH+ grafted cells. Young rats had greater neurite outgrowth on a per grafted cell basis compared to both middle aged and aged grafted rats. The asterisk denotes significant difference between young versus middle aged and aged groups ($p < 0.05$).

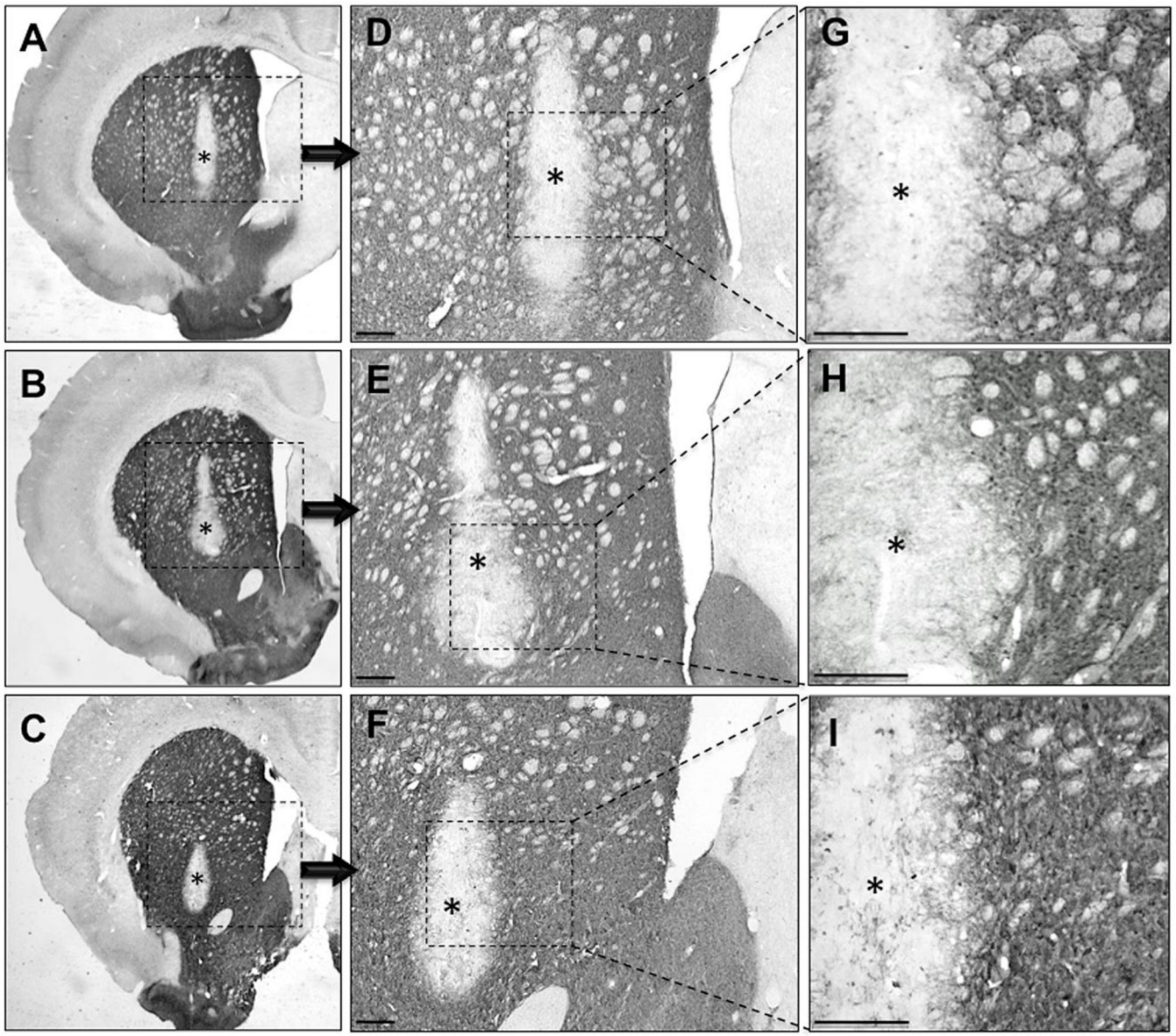

Figure 5.

Representative photomicrographs of striatal DARPP-32 staining in young (**A, D, G**), middle-aged (**B, E, H**), and aged (**C, F, I**) rats with intrastriatal DA neuron grafts (*asterisk). These images show that the graft protocol used resulted in an equivalent, relatively small area of disruption of DARPP-32 positive neurons across the various host age groups despite varying degrees of TH+ graft number and infiltration into the host striatum. Quantification data of the percent of striatal volume devoid of DARPP-32+ immunoreactivity showed no age-related difference in the volume of striatum staining for DARPP-32 (VM grafted rats: young 99.85% ± 0.86; middle-aged 98.30% ± 0.57; aged 96.93% ± 0.473; % of striatal volume with DARPP-32-ir; $F(2,36.)=1.18$, $p > 0.05$) and equivalent to the volume of DARPP-32 staining in sham-grafted rats (sham-grafted rats: young 99.97% ± 0.75; middle-aged 99.95% ± 0.53; age 99.97% ± 0.669). Scale bars represent 100 μm.

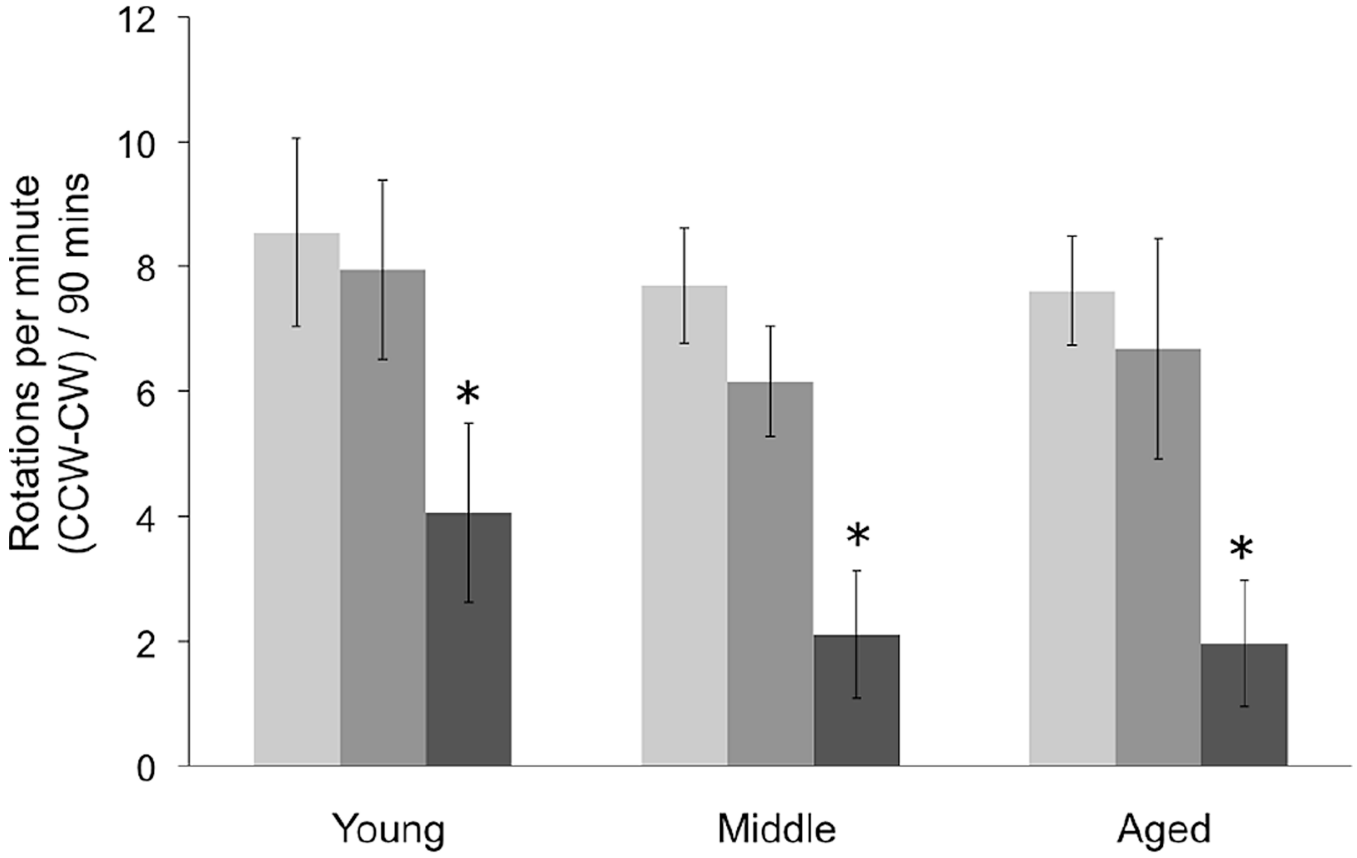

Figure 6.

Lesion and graft efficacy measured with amphetamine-induced rotational behavior. Experimental groups: Light gray bars= Baseline Pre-graft; Mid-tone gray bars= Sham-grafted rats 10 weeks post grafting; Dark gray bars= VM grafted rats 10 weeks post grafting. Asterisk denotes significant difference between VM graft animals versus baseline pre-graft and sham-graft scores ($p < 0.05$). CCW= counter clockwise turn; CW=clockwise turn.

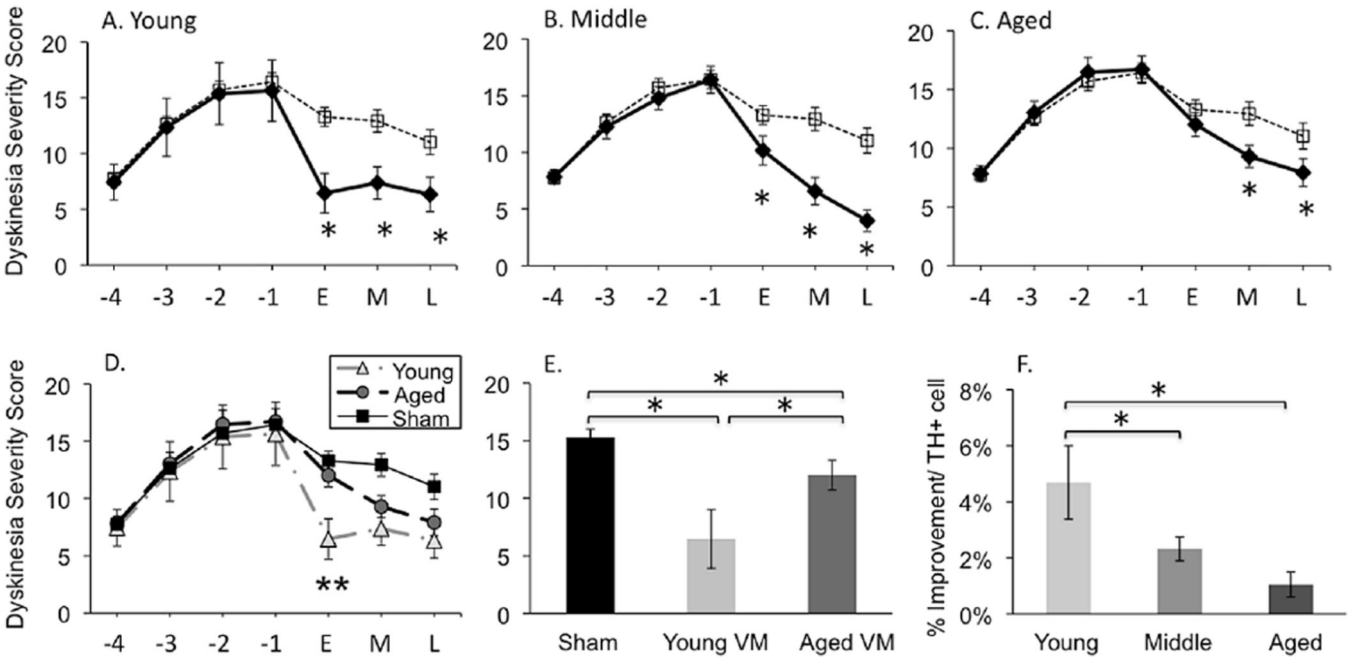

Figure 7.

Comparison of 'total' levodopa-induced dyskinesias severity across ages (**A-C**). Sham grafted rats: dashed line; VM grafted rats: solid line. The asterisks denotes significant difference between VM and sham grafted groups at $p < 0.05$. (**D**) Illustration of 'total' levodopa-induced dyskinesias in young and aged VM grafted and sham-grafted rats across all time points. The double asterisk denotes significant difference between young and aged VM graft groups at $p < 0.05$. (**E**) Total dyskinesias severity comparison between sham-grafted, young VM grafted, and aged VM grafted animals at early ('E'; 2–4 week) post graft time point. The asterisks denotes significant differences ($p < 0.05$) for indicated comparison. (**F**) Percent improvement in dyskinesias severity per grafted TH+ cell number. The asterisks denotes significant differences ($p < 0.05$) for indicated comparison. X-Axis: −4, −3, −2, −1 are pre-grafting time points (in weeks) where levodopa priming occurred. 'E'= early, 'M'= middle, 'L'= late, are post-graft time points determined using modified boot-strapping statistics with the 'E' time-point = weeks 2–4 wks post-grafting; the M time-point = weeks 6–8 wks post-grafting; and the 'L' time-point weeks =10–11 wks post-grafting. Daily levodopa treatment continued post-grafting as detailed in Figure 1.

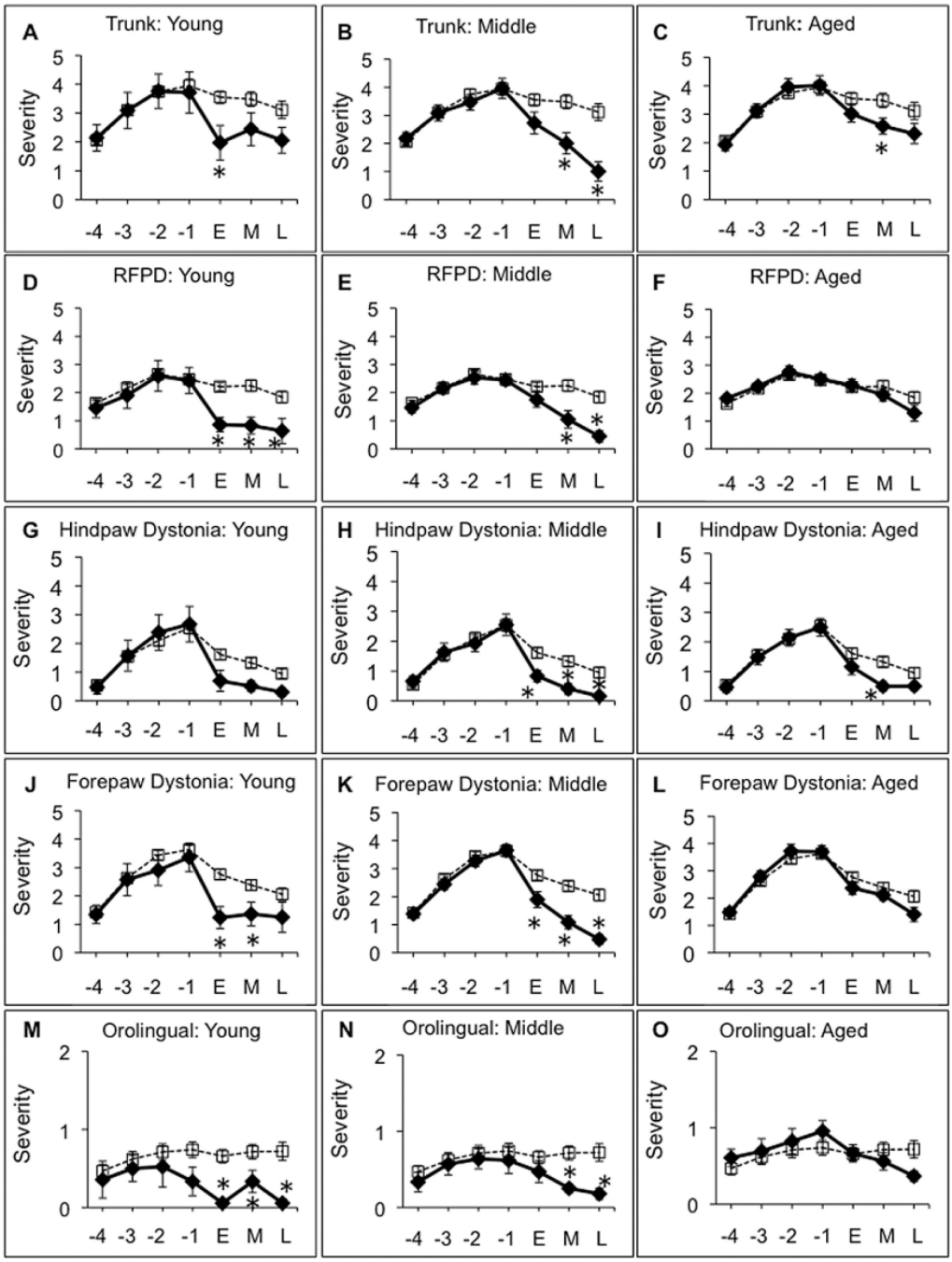

Figure 8.

Individual attributes of levodopa-induced dyskinesias for young (**A, D, G, J, M**), middle-aged (**B, E, H, K, N**), and aged (**C, F, I, L, O**) rats at pre-graft and post-graft time points. Trunk (**A-C**), Right Fore Paw Dyskinesia (RFPD) (**D-F**), hind paw (**G-I**), forepaw (**J-L**), orolingual (**M-O**). The dashed line represents sham-grafted rats. The solid line represents VM grafted rats. *X-Axis:* −4, −3, −2, −1 are pre-grafting time points (in weeks) where levodopa priming occurred. 'E'= early, M= middle, 'L'= late, are post-graft time points determined using modified boot-strapping statistics with the 'E' time-point = weeks 2–4 wks

post-grafting; the ‘M’ time-point = weeks 6–8 wks post-grafting; and the ‘L’ time-point weeks =10–11 wks post-grafting. The asterisks denotes significant differences ($p < 0.05$) at indicated time point for sham versus VM graft groups.

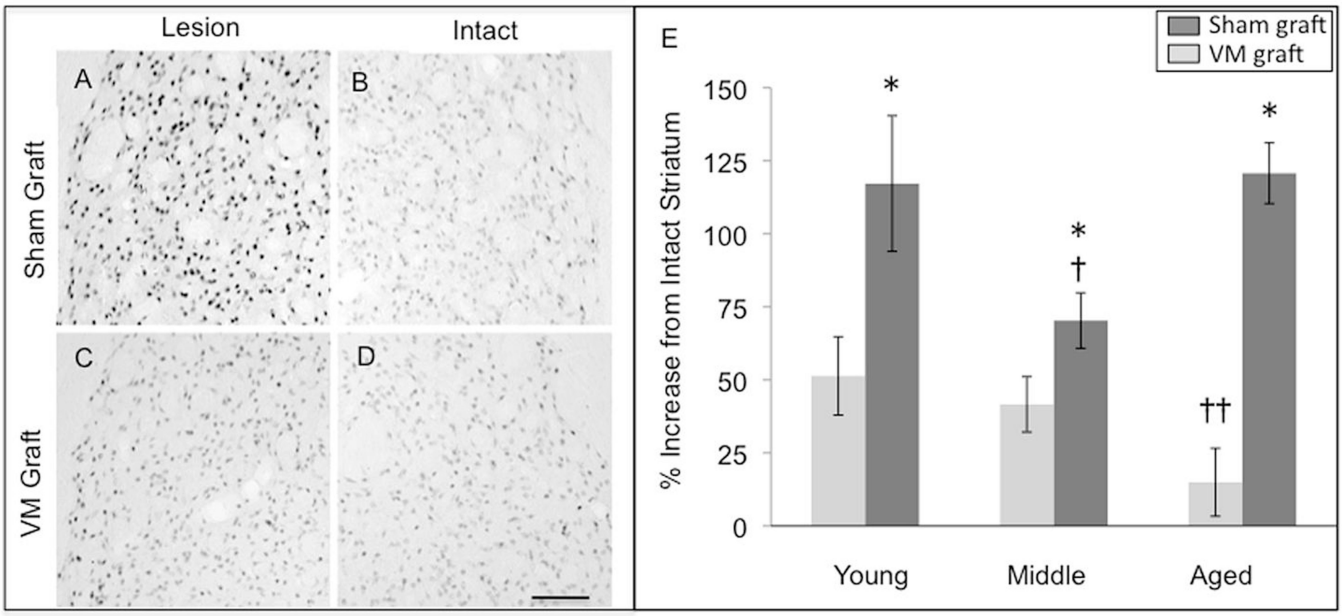

Figure 9.

Densitometric quantitation of FosB/ΔFosB immunohistochemistry in sham and VM grafted rats. (A–B) A representative example of the elevated density of FosB/ΔFosB immunostaining in the lesioned, DA-depleted striatum of a young sham-grafted rat treated with chronic levodopa compared to that in the contralateral intact striatum. (C–D) As seen in ‘C the presence of a VM graft significantly reduced the elevation in FosB/ΔFosB as shown in this representative example from a young rat. (E) The elevation of FosB/ΔFosB densitometry in the sham grafted striatum (dark gray bars) occurred in all age groups, however, the elevation was significantly less in the middle aged group compared to both the young and aged groups († $p<0.05$). The presence of a VM graft (light gray bars) reduced FosB/ΔFosB densitometry across all age groups with the reduction greatest in aged rats with the largest grafts; †† indicates significant difference between the aged VM grafted group and the young and middle aged VM grafted groups ($p<0.05$). A single asterisk (*) indicates significant difference between sham vs. VM graft within that age group ($p<0.05$). Scale bar represents 100 μm for A–D.

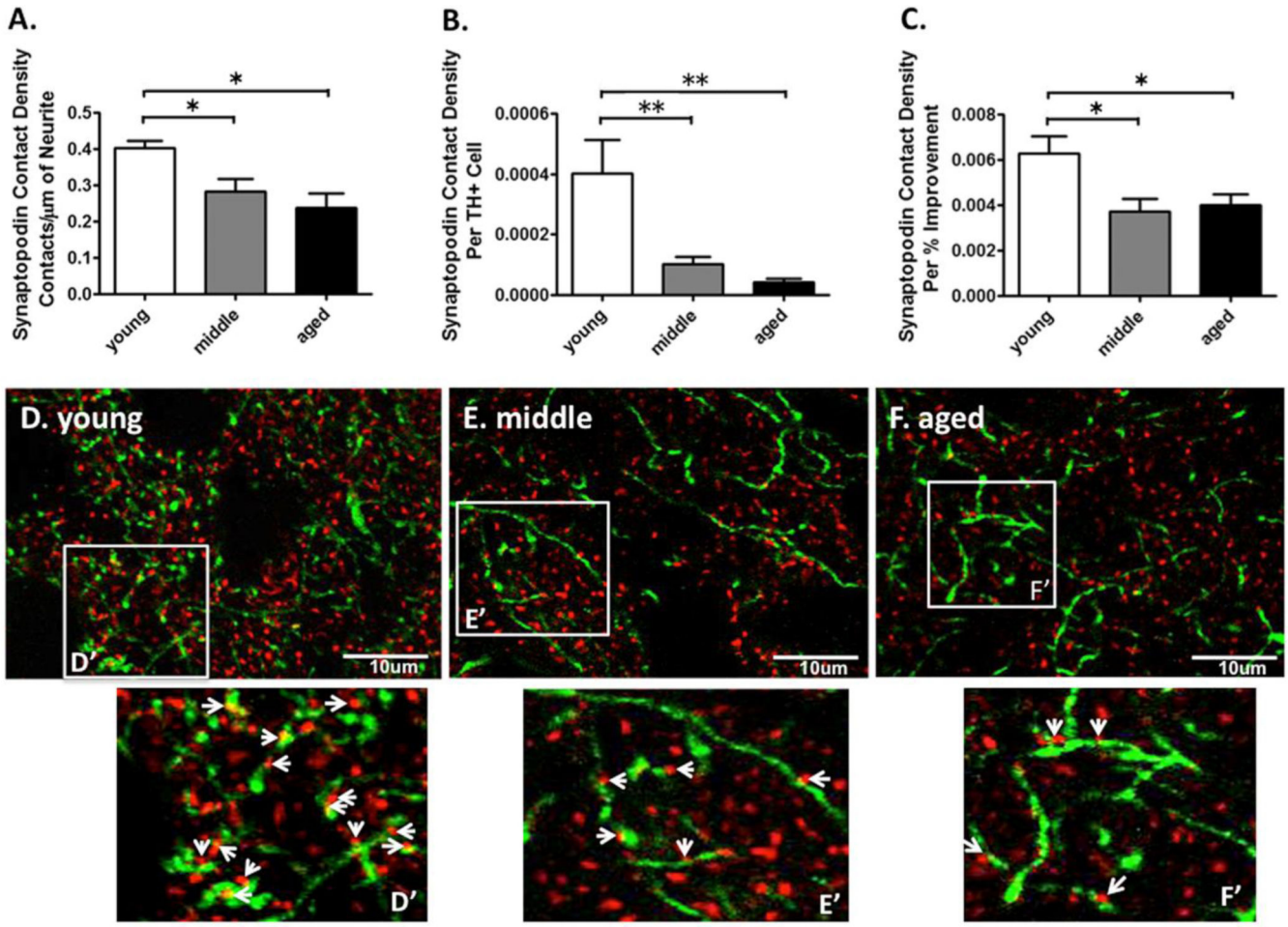

Figure 10.

Measurements of synaptic contacts formed between tyrosine hydroxylase (TH)+ neurites in the VM graft and synaptopodin (SP)+ dendritic spines of host MSNs in young, middle aged, and aged rats. (A) The SP contact density (i.e.: the number of contacts with SP+ spines per 10µm TH+ neurite) was greater for young VM grafted vs. middle aged and aged VM grafted rats. The asterisk denotes $p<0.05$ for the indicated comparison. (B) The SP contact density per surviving grafted dopaminergic neuron was greater for young VM grafted vs. middle aged and aged VM grafted rats. The double asterisk denotes $p < 0.01$ for the indicated comparison. (C) The SP contact density per percent reduction in LID severity post grafting was greater for young VM grafted vs. middle aged and aged VM grafted rats. The asterisk denotes $p < 0.05$ for the indicated comparison. (D–F) Representative photomicrographs of dual-label immunohistochemistry for DA neurites (TH, green) and spines of host MSNs (SP, red) in young (D), middle (E), and aged (F) VM grafted rats. (D'-F') Enlarged images show the number of presumed synaptic contacts (arrows) formed between TH+ neurites and SP+ spines.